iScience

CellPress
OPEN ACCESS

Article

Red blood cell signaling is functionally conserved in *Plasmodium* invasion

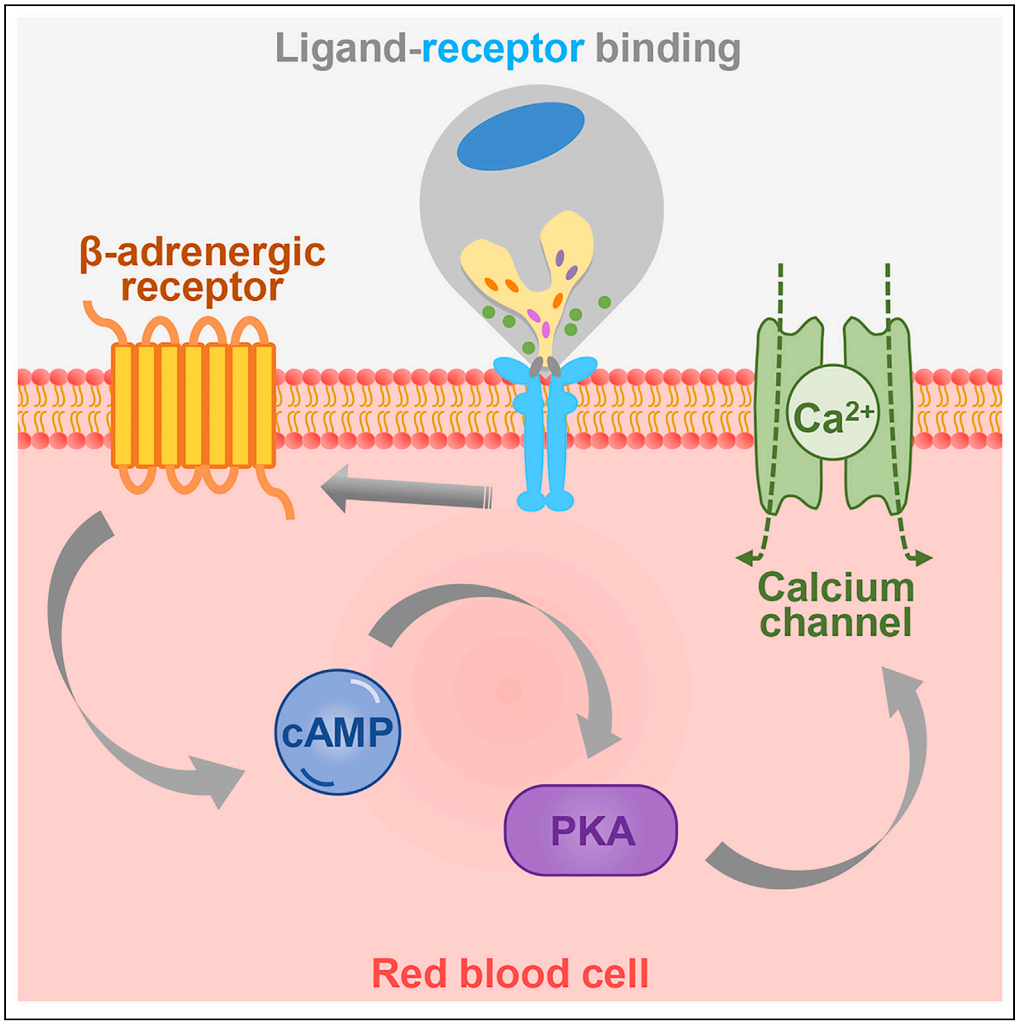

James Jia Ming Yong, Xiaohong Gao, Prem Prakash, ..., Julien Lescar, Hoi Yeung Li, Peter R. Preiser

prpreiser@ntu.edu.sg

Highlights

RBC calcium signaling is conserved in *Plasmodium* invasion

RH5-basigin interaction modulates host cAMP dynamics

RH5-basigin associated complex triggers host cAMP singling required for invasion

Yong et al., iScience 27, 111052
October 18, 2024
https://doi.org/10.1016/j.isci.2024.111052

iScience

CellPress
OPEN ACCESS

Article

Red blood cell signaling is functionally conserved in *Plasmodium* invasion

James Jia Ming Yong,[1,2] Xiaohong Gao,[1,2] Prem Prakash,[1,3] Jing Wen Ang,[1] Soak Kuan Lai,[1] Ming Wei Chen,[1] Jason Jun Long Neo,[1] Julien Lescar,[1] Hoi Yeung Li,[1] and Peter R. Preiser[1,4,*]

SUMMARY

It is widely recognized that *Plasmodium* merozoites secrete ligands that interact with RBC receptors. Meanwhile the question on whether these interactions trigger RBC signals essential for invasion remains unresolved. There is evidence that *Plasmodium falciparum* parasites manipulate native RBC Ca^{2+} signaling to facilitate invasion. Here, we demonstrate a key role of RBC Ca^{2+} influx that is conserved across different *Plasmodium* species during invasion. RH5-basigin interaction triggers RBC cAMP increase to promote Ca^{2+} influx. The RBC signaling pathways can be blocked by a range of inhibitors during *Plasmodium* invasion, providing the evidence of a functionally conserved host cAMP-Ca^{2+} signaling that drives invasion and junction formation. Furthermore, RH5-basigin binding induces a pre-existing multimeric RBC membrane complex to undergo increased protein association containing the cAMP-inducing β-adrenergic receptor. Our work presents evidence of a conserved host cell signaling cascade necessary for *Plasmodium* invasion and will create opportunities to therapeutically target merozoite invasion.

INTRODUCTION

Malaria is a major burden in developing countries today, resulting in more than 500,000 deaths each year. While *Plasmodium falciparum* infection remains the deadliest form of malaria, zoonotic malaria represents a public health concern in Southeast Asia by which *Plasmodium knowlesi* has emerged as the predominant human-infecting *Plasmodium* species.[1] *Plasmodium* merozoites possess distinct repertoires of reticulocyte binding protein homologues (RHs) and erythrocyte binding-like proteins (EBLs) to bind to their respective RBC surface receptors and direct invasion.[2–10] Moreover, RBCs respond to molecular cues from *Plasmodium* merozoites by eliciting specific signaling events and modulating membrane deformability[11,12] critical for invasion, highlighting that the host is not a passive bystander but an active player in the invasion process.

To date, little is known about the functional roles of the RBC in invasion. It has been shown that the RBC possesses innate signaling pathways which adaptively regulate its structural, metabolic, and transport functions in response to external stimuli and stress conditions.[13–15] A major indication of RBC involvement in *Plasmodium* invasion was first reported by Weiss et al., in which they highlight that extracellular Ca^{2+} is critical for RBC signaling during invasion. Our previous studies have identified that the binding of RH5 to basigin triggers extracellular Ca^{2+} influx in the RBC leading to cytoskeleton protein phosphorylation that alters the overall RBC cytoskeleton architecture required for invasion.[11] This is consistent with the importance of Ca^{2+} signaling in mediating RBC cytoskeleton protein changes under physiological conditions and pathological alteration which is associated with various diseases such as sickle cell anemia.[13,16] Though our understanding on how RH5-basigin interaction induces extracellular Ca^{2+} uptake or the signaling molecules triggered by RH5 prior to RBC cytoskeleton modulation remains limited, the characteristic RBC Ca^{2+} influx strongly implies that the parasite has manipulated native RBC signaling pathways to drive successful invasion. Above all, in the broader perspective of elucidating the host cell mechanisms in invasion, it remains unclear whether similar RBC signaling pathways play a conserved and critical role across species, considering that RH5 is only expressed in *P. falciparum* strains.

cAMP-dependent protein kinases (PKAs) are crucial in the activation of Ca^{2+} transporters that permit the entry of extracellular Ca^{2+} involved in mediating key biological functions in various mammalian cells.[17–19] Conventional cAMP signaling involves the activation of beta-2 adrenergic receptor (β2AR) by heterotrimeric G proteins (αβγ subunits), leading to the dissociation of stimulatory G protein α (Gαs) that stimulates membrane-associated adenylyl cyclase (AC) to catalyze the cyclization of ATP into cAMP.[20–22] Elevated levels of intracellular cAMP then interact with the PKA regulatory subunits (PKAr), releasing activated PKA catalytic subunits (PKAc) that phosphorylate the serine and threonine residues on its effector proteins.[23] Interestingly, pre-existing cAMP signaling proteins and Ca^{2+} channels in the RBC intertwine in molecular interactions to mediate changes in RBC biomechanics such as membrane deformation.[24] Furthermore, PKA and

[1]School of Biological Sciences, Nanyang Technological University, 60 Nanyang Drive, Singapore 637551, Singapore
[2]These authors contributed equally
[3]Present address: Center for Global Health and Infectious Disease Research, College of Public Health, University of South Florida, 3720 Spectrum Boulevard, Tampa, Florida 33612, USA
[4]Lead contact
*Correspondence: prpreiser@ntu.edu.sg
https://doi.org/10.1016/j.isci.2024.111052

Ca^{2+}-dependent kinases are known to phosphorylate RBC cytoskeleton proteins, such as adducin and protein 4.1R, and induce the destabilization of the cytoskeletal network in line with our previous findings on the significant loss of ankyrin and adducin and increase in the RBC spectrin mesh size upon RH5 binding.[11,25,26] However, whether *Plasmodium* merozoites exploit these RBC cAMP-Ca^{2+} signaling events to facilitate downstream cytoskeleton protein phosphorylation in invasion is unknown.

Here we demonstrated the conservation of RBC Ca^{2+} signaling in three *Plasmodium* species in invasion: *P. falciparum* (human), *P. knowlesi* (human), *P. knowlesi* (macaque), and the rodent-infecting *P. yoelii* (mouse), suggesting the existence of a universal invasion phenomenon across *Plasmodium* species in which the interaction between species-specific invasion ligands and their respective host receptors eventually converges to a common host cell derived signaling cascade, further highlighting that the active involvement of RBC signaling pathways is mandatory for *Plasmodium* invasion. Furthermore, we provided evidence that the inhibition of cAMP signaling proteins and L-type Ca^{2+} channels, one of the major voltage-gated Ca^{2+} channels, effectively blocked *P. falciparum* and *P. knowlesi* merozoite invasion and impeded junction formation, indicating that a host cAMP-Ca^{2+} signaling crosstalk is functionally conserved and governs junction formation in *Plasmodium* invasion. We have also dissected the molecular events in a host cell derived signaling cascade upon RH5-basigin binding: RH5-bound basigin associates with a multimeric RBC membrane complex which undergoes increased assembly and recruitment of RBC proteins including the cAMP-inducing β2AR, and subsequently triggers a rise in RBC cytosolic cAMP levels necessary for extracellular Ca^{2+} uptake via RBC L-type Ca^{2+} channels ahead of junction formation. Taken together, our study provides the functional context for the key role of a conserved RBC cAMP-Ca^{2+} signaling crosstalk across *Plasmodium* species. These findings have broad implications about how *Plasmodium* merozoites exploit innate RBC signaling mechanisms and molecular players to drive the invasion process, thereby providing further insights into potential targets for drug intervention.

RESULTS

Ca^{2+} signaling in the RBC is functionally conserved in *Plasmodium* invasion

Merozoite invasion is a key step of the *Plasmodium* parasite's life cycle. In all *Plasmodium* species, merozoite-encoded proteins contribute to the invasion process by facilitating the attachment and entry of the merozoite to the RBC.[6,10,27] While our previous findings have indicated that the binding of RH5 to basigin triggers RBC Ca^{2+} signaling,[11] it is unknown whether the host cell signaling event is restricted to *P. falciparum* or conserved across *Plasmodium* spp. and whether it is essential for successful invasion. Ca^{2+} is an ubiquitous messenger ion in mammalian cells including myocytes, neurons and secretory epithelial cells, and RBCs possess native Ca^{2+}-dependent signaling pathways to regulate key functions under physiological conditions.[13,14,17,18,24] EGTA is a cell impermeable, extracellular Ca^{2+} chelator. It has been shown that depletion of extracellular Ca^{2+} by EGTA does not affect intracellular Ca^{2+} levels and microneme discharge of the merozoite,[28] suggesting that the parasite utilises internal Ca^{2+} stores to facilitate invasion. Therefore, this raises the possibility that *Plasmodium* merozoites exploit pre-existing host Ca^{2+}-dependent signaling pathways to invade RBCs. Importantly, Ca^{2+} removal from the media using EGTA blocks both *P. falciparum* and *P. knowlesi* merozoite invasions (Figure S1A), highlighting that external Ca^{2+} is essential for *Plasmodium* invasion, which is in line with the previous studies.[29,30] To investigate whether RBC Ca^{2+} signaling is conserved in non-*falciparum* merozoite invasion, we performed live video microscopy by using *P. falciparum* 3D7, *P. knowlesi* A1-H.1 and *P. yoelii* YM with Fluo-4a.m. labeled RBCs from human, macaque, and BALB/cN mouse, respectively. The snapshots clearly showed successful invasions that begin with a detectable Ca^{2+} influx in the host cell after merozoite initial attachment and reorientation, and the Ca^{2+} signal rapidly spreads throughout the entire RBC (Figure 1, Videos S1, S2, S3, and S4). Subsequently, the invaded RBCs similarly exhibited massive deformation and Ca^{2+} decrease over time. This is further confirmed by RBC Ca^{2+} measurement showing that *P. falciparum* 3D7 (in human) and *P. knowlesi* A1-H.1 (in human and monkey) invasions trigger RBC Ca^{2+} signaling (Figures S1B–S1D). These data expand on our previous findings that RH5-basigin interaction triggers RBC Ca^{2+} signaling during *P. falciparum* invasion by showing that RBC Ca^{2+} signaling is a functionally conserved invasion step in other *Plasmodium* species is induced by species-specific ligand-receptor interactions.

RH5-basigin binding triggers a rise in RBC cAMP level to direct RBC Ca^{2+} signaling

cAMP is a second messenger, transducing the cAMP-dependent pathway in multiple biological processes. The basal level of cAMP in the cell is about 1 μM and the levels change up to around 20-fold after stimulation in cells such as neurons, myocytes, and pathogens.[31–33] Mammalian RBCs lack intracellular Ca^{2+} stores and tightly regulate RBC Ca^{2+} uptake via stimulated membranous Ca^{2+} transporters to maintain low intracellular Ca^{2+} concentrations.[13,34,35] The activation of the cAMP-PKA pathway is associated with Ca^{2+} influx through Ca^{2+} channels in mammalian cells and is in line with pre-existing interactions between the cAMP and Ca^{2+} signaling pathways occurring in RBCs to permit the entry of Ca^{2+} that regulate biomechanical properties of the RBC membrane and adapt to extracellular signals in the blood microenvironment.[13,24,36] To address whether the binding of parasite ligand to host receptor triggers cAMP signaling in the RBC during invasion, we have successfully purified full-length recombinant RH5 protein with His-tag (rRH5) in an expected size of 63 kDa (Figure S2A) as described previously.[11] Properly folded rRH5 directly binds to RBC in the erythrocyte binding assay, confirming that rRH5 acts as native RH5 in line with our previous studies (Figure S2B).[11] We utilized rRH5 to measure the dynamic changes of RBC cAMP levels upon rRH5 binding using a cAMP competitive enzyme-linked immunosorbent assay (ELISA). The RBC cAMP level in the absence of rRH5 was used as a negative control. Forskolin, an AC activator, elevated intracellular cAMP levels rapidly (Figure 2A). On the addition of RH5, there is a significant rise in cAMP levels to the peak of 10.63 μM at about 2 min that decreases to 5.27 μM after 10 min, suggesting that RH5 triggers a transient increase of RBC intracellular cAMP levels (Figure 2A). Importantly, this transient RBC cAMP increase can be effectively inhibited by anti-basigin Fab fragment, highlighting that the RH5-basigin interaction is required for RBC cAMP signaling (Figure 2B). Furthermore, the observed peak in cAMP levels at 2 min can be blocked by

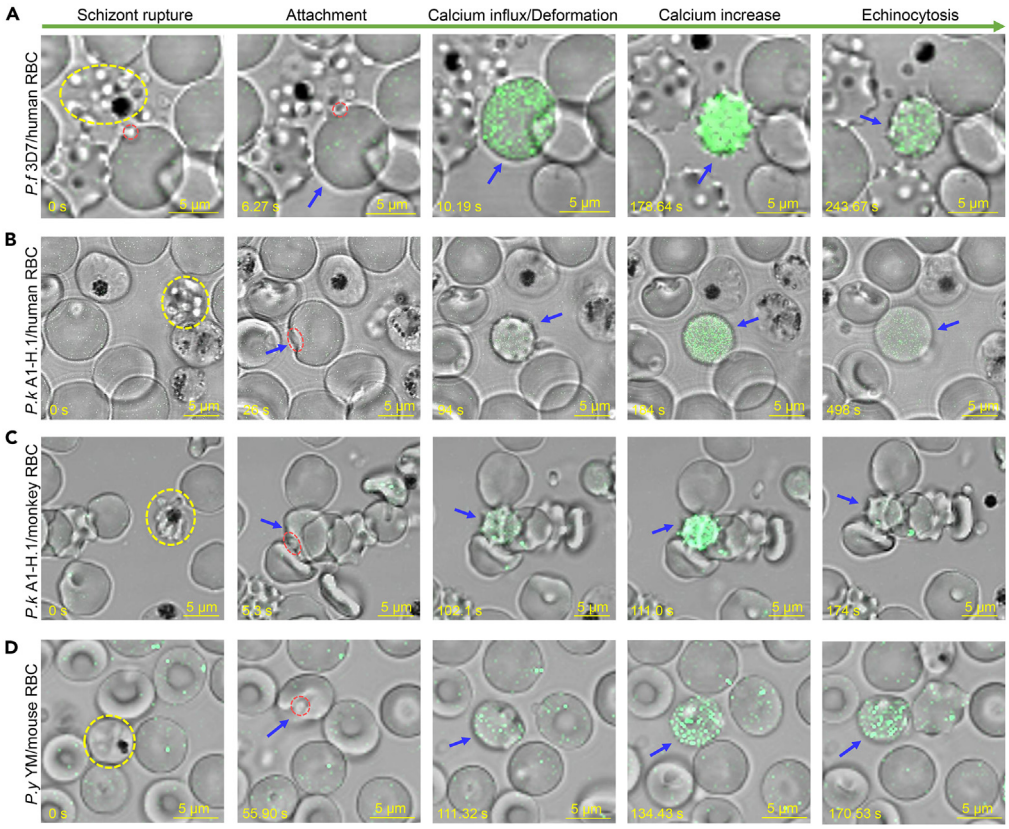

Figure 1. Ca^{2+} signaling is captured during *Plasmodium* merozoite invasion

Normal RBCs of human, monkey and mouse were loaded with Fluo-4a.m. Representative video snapshots were taken for *P. falciparum* 3D7 (A) *P. knowlesi* A1-H.1 (B and C) and *P. yoelii* YM (D) invading their respective labeled host RBCs, respectively. Merozoite (dotted circle in red) attaches to the RBC (arrow in blue) after the schizont rupture (dotted circle in yellow) and reorients followed by Ca^{2+} influx that spreads throughout the entire RBC. The Ca^{2+} influx causes a massive deformation, and the signal starts to decrease when echinocytosis happens (Videos S1–S4). Relative time was shown in seconds. Scale bar = 5 µm.

permeable G protein inhibitor BIM46187 and AC inhibitor 2′,5′-ddA (Table 1; Figure 2B), confirming that RH5-basigin interaction triggers RBC cAMP generation.

To directly validate the relationship between RH5-basigin interaction and the changes in cytosolic cAMP level in the RBC, a cAMP-sensing fluorescent biomolecule with real-time tracking properties would enable time-resolved measurement of RBC cAMP dynamics during invasion. Harada et al. has demonstrated a cAMP-sensing indicator protein termed Pink Fluorescent cAMP indicator (Pink Flamindo) that is able to specifically detect cAMP molecules and monitor spatiotemporal intracellular cAMP dynamics by exhibiting an increase in fluorescence intensity upon cAMP binding.[49] Since most proteins cannot passively diffuse across the plasma membrane due to their size and polarity,[50] this suggests that a soluble Pink Flamindo protein can be loaded inside RBCs as a cAMP biosensor to track RBC cAMP levels in response to the binding of invasion ligands. A recombinant N-terminal His- and thioredoxin-tagged Pink Flamindo protein was generated and verified by SDS-PAGE and western blot. Two protein band sizes at approximately 45 kDa and 57 kDa (Figure S2C) were visualized using Coomassie blue staining.[49,51,52] Furthermore, ~57 kDa full-length Pink Flamindo protein was detected by using anti-His antibody (Ab) (Figure S2D). Fresh RBCs were preloaded with Pink Flamindo, using a modified protocol from Murphy et al.[53] and termed "Resealed RBC" (rRBC). Influenza Hemagglutinin (HA) peptide was also loaded into rRBCs as an internal control and shown by dot blot assay using anti-HA antibody to be specifically captured within these resealed RBCs (Figure S3A), while no signal was detected in Empty rRBCs thereby validating this approach. We can now take full advantage of this lysis-resealing method to detect cAMP signals in Pink Flamindo loaded rRBCs. To examine whether rRBCs loaded with Pink Flamindo are able to report intracellular cAMP dynamics, direct visualisation of induced RBC cAMP increase using fluorescent microscopy was carried out. Pink Flamindo loaded rRBC alone was used as a negative control (Figure 2Ci). In line with cAMP competitive ELISA mentioned above, both rRH5 and forskolin induce the increase in RBC cytosolic cAMP with most cells exhibiting strong red signals (Figures 2Cii and 2Ciii). In contrast, anti-basigin Fab fragment, BIM46187 and 2′,5′-ddA significantly decreased the number of red fluorescent RBCs upon rRH5 binding (Figures 2Civ–2Cvi). Interestingly, neither PKA inhibitor PKA (14–22) nor L-type Ca^{2+} channel inhibitor verapamil (Table 1) was able to prevent red cAMP signal increase in the RBC in the presence of rRH5 (Figures 2Cvii and 2Cviii). Moreover, rRH5-induced RBC cAMP signal was quantified by using fluorescent plate reader. Accumulative cAMP signals were obtained at 600 s and graphically represented as a bar chart in Figure 2D. As expected, both rRH5 and forskolin trigger RBC cAMP increase, while Fab,

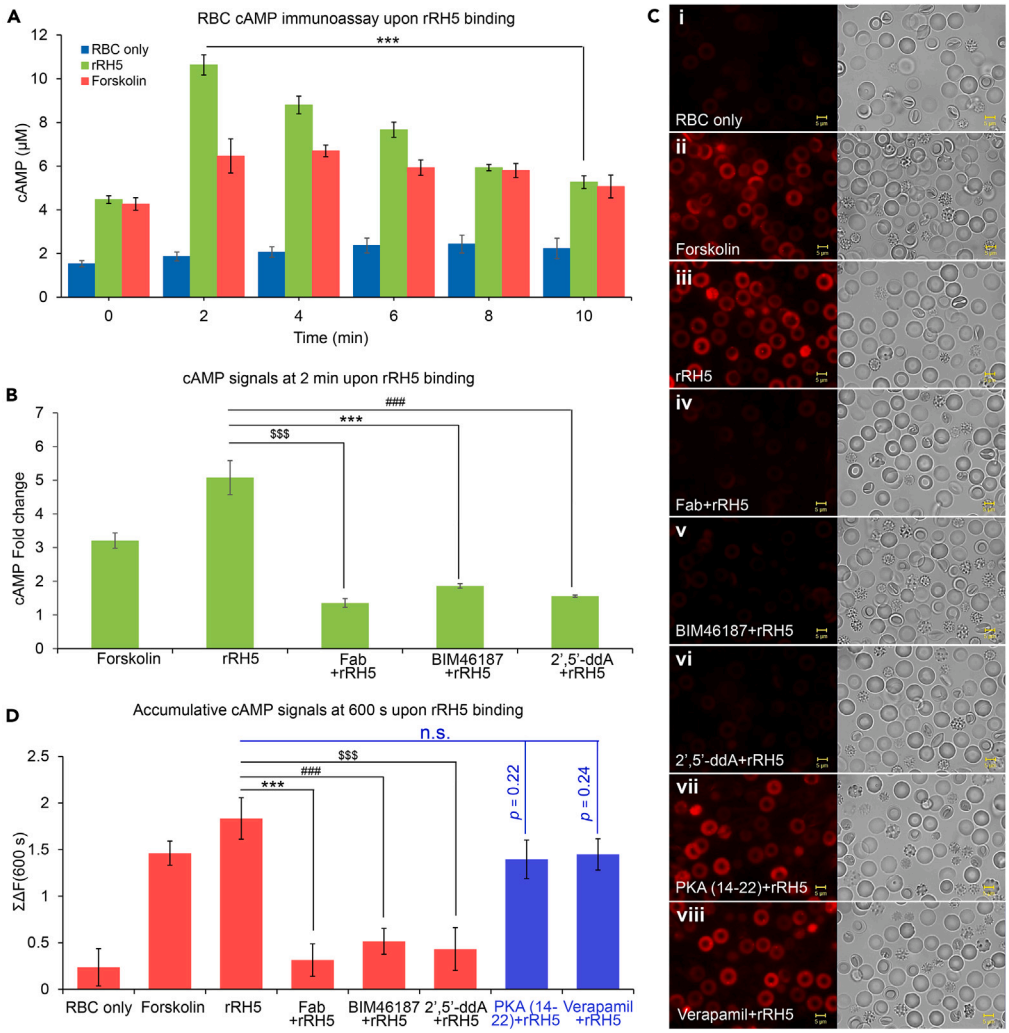

Figure 2. RH5-basigin interaction triggers a rise in cytosolic cAMP level

Recombinant rRH5 was purified and used for all the assays.

(A) cAMP immunoassay of RBCs was carried out. The dynamic changes of RBC cAMP level were measured in the absence (RBC only) and presence of 0.2 mg/mL rRH5 protein (RH5) within 10 min in 2-min intervals. Forskolin was used as a positive control (Forskolin). Experimental data presented as mean ± s.e.m, $n = 3$. ***$p = 0.0006$ indicates the significant difference on the cAMP level at 2 min compared to that at 10 min.

(B) cAMP inhibition immunoassay of RBCs. The dynamics of RBC cAMP level was measured upon rRH5 binding for 2 min in the absence (RH5) and presence of anti-basigin Fab fragment (Fab+rRH5), G protein inhibitor BIM46187 (BIM46187+rRH5) or AC inhibitor 2′,5′-ddA (2′,5′-ddA + rRH5). Forskolin was used as a positive control (Forskolin). The cAMP reading in RBC alone was used as a negative control. The fold change in cAMP level in the samples was compared to that in the negative control and plotted as a bar chart. $$$$p = 0.002$, ***$p = 0.003$ and ###$p = 0.002$ indicate the significant difference on fold change in RBC cAMP level upon rHR5 binding between in the absence (rRH5) and presence of anti-basigin Fab fragment (Fab+rRH5), BIM46187 (BIM46187+ rRH5) or 2′,5′-ddA (2′,5′-ddA + rRH5), respectively. Experimental data presented as mean ± s.e.m, $n = 3$.

(C) Fluorescence images of RBC cAMP. Pink Flamindo loaded rRBCs were incubated in the absence (i, RBC only) and presence of forskolin (ii, Forskolin), rRH5 (iii, rRH5), anti-basigin Fab fragment (iv, Fab+rRH5), BIM46187 (v, BIM46187+rRH5), 2′,5′-ddA (vi, 2′,5′-ddA + rRH5), PKA (14–22) (vii, PKA (14–22)+rRH5) or verapamil (viii, Verapamil+rRH5) prior to rRH5 binding for 10 min. Fluorescence (left) and bright field (right) images were taken under 100× objective lens. Scale bars = 5 μm.

(D) RBC cAMP measurement by using fluorescence plate reader. The cAMP signal intensity of the samples obtained from (C) were also measured. Dynamics of RBC cytosolic cAMP level was measured over 600 s ΣΔF(t) which reflects the cumulative change in RBC cytosolic cAMP was plotted as a bar chart. ***$p = 0.006$, ###$p = 0.007$, and $$$$p = 0.012$ indicate the significant difference in RBC cAMP level upon rHR5 binding between in the absence (rRH5) and presence of anti-basigin Fab fragment (Fab+rRH5), BIM46187 (BIM46187+ rRH5) or 2′,5′-ddA (2′,5′-ddA + rRH5), respectively. Whereas no significant inhibition effect was seen in PKA (14–22) or Verapamil with $p > 0.05$ (n.s.) including $p = 0.22$ and $p = 0.24$ (color in blue). Experimental data presented as mean ± s.e.m, $n = 3$. Statistical comparison was done using one-way ANOVA.

Table 1. Properties of signaling inhibitors used in the merozoite invasion inhibition assays and RBC cAMP-Ca^{2+} signaling assays

Permeability	Compounds	Abbreviation	Company	Target	Reference
Membrane-permeable	BIM46187	–	MedChem Express	G protein	Ayoub et al.[37]
	2′,5′-Dideoxy-adenosine	2′,5′-ddA	Sigma	AC	Bitterman et al.[38]
	PKA (14–22)	–	Sigma	PKAc	Swierczewski et al.[39]
	Verapamil	–	Sigma	L-type Ca^{2+} channels	Catterall et al.[40]
Membrane-impermeable	G Protein antagonist peptide	GPA	Sigma	βAR	Mukai et al.[41] Somvanshi et al.[42]
	NF449	–	Santa Cruz Biotechnology	Gαs	Guo et al.[43]
	2′-Deoxy-adenosine 3′-monophosphate	2′-*d*-3′-AMP	Santa Cruz Biotechnology	AC	Tesmer et al.[44]
	Rp-8-OH-cAMPS	–	Santa Cruz Biotechnology	PKAr	Chu et al.[45]
	PKA (6–22)	–	Sigma	PKAc	Dalton et al.[46] Glass et al.[47]
	N-methyl verapamil	N-methyl Vera	Abcam	L-type Ca^{2+} channels	Zhang et al.[48]

BIM46187 and 2′,5′-ddA significantly block the RBC cAMP signal which is consistent with the fluorescent images (Figure 2D, bar chart in red), confirming that Pink Flamindo as a cAMP indicator is able to track RH5-induced RBC cAMP increase. Both PKA and L-type Ca^{2+} channel inhibitors were not able to block the cAMP increase upon rRH5 binding which are related to images in Figures 2C, 2Cvii, and 2Cviii, (Figure 2D, bar chart in blue), suggesting that these proteins function downstream of the cAMP-synthesizing AC and require the presence of a cytosolic cAMP pool for activation. Taken together, these data demonstrate that RH5-basigin binding is able to trigger RBC cAMP signaling and in turn elevate the host intracellular cAMP concentration.

To further examine whether an elevated cAMP level regulates extracellular Ca^{2+} uptake into the RBC, direct visualization of induced RBC Ca^{2+} increase using fluorescent microscopy and fluorescent plate reader were carried out. Accumulative Ca^{2+} signals were obtained at 600 s and graphically represented as a bar chart in Figure 3B. Fluo-4 a.m. labeled RBC alone was used as a negative control with only few cells fluorescing (Figure 3Ai). In line with our previous findings, rRH5 triggers the increase of RBC cytosolic Ca^{2+} that causes the whole RBC to fluoresce (Figures 3Aii). In contrast, both BIM46187 and 2′,5′-ddA significantly decreased the number of RBCs that fluoresces upon rRH5 binding (Figures 3Aiii and 3Aiv), which is consistent with the plate reader data (Figure 3B, bar chart in green), confirming that cAMP triggered by RH5 binding is directly linked to RBC Ca^{2+} increase. Moreover, PKA (14–22) and verapamil (Table 1) also dramatically reduced the number of RBCs that fluoresces in the presence of rRH5 (Figures 3Av, 3Avi, and 3B, bar chart in blue), providing clear evidence of a signaling cascade involving cAMP, PKA and L-type Ca^{2+} channels.

Notably, all inhibitors mentioned above for the rRH5-based experiments are membrane-permeable. As parasite encoded cAMP signaling molecules, such as β2AR, AC, and PKA, are also essential for parasite growth, survival, egress, and invasion,[54] it is critical that the inhibitors used to analyze the host cell signaling molecules during invasion must not interfere with signaling proteins in the parasite. Hence, for merozoite-based experiments, membrane-impermeable inhibitors (Table 1) that are trapped in the confines of the RBC membrane and do not lead to off-target inhibition on the merozoite during invasion were used. To achieve this, RBCs were preloaded with each impermeable inhibitor of interest using the lysis-resealing method protocol as described. Importantly, resealed RBCs are invaded with equal efficiency as normal RBCs (Figures S3B–S3C), indicating that the resealed RBCs can be used for merozoite invasion-related studies. To assess whether the impermeable signaling inhibitors have any effect on the merozoite, merozoite invasion assays were carried out using normal intact RBCs in the presence of impermeable βAR inhibitor GPA, Gαs inhibitor NF449, AC inhibitor 2′-*d*-3′-AMP, PKAr inhibitor Rp-8-OH-cAMP, PKAc inhibitor PKA (6–22) or L-type Ca^{2+} channel inhibitor N-methyl Vera (Table 1) in the culture media. Of note, none of the inhibitors showed significant inhibitory effect on invasion as compared to the untreated control (Figure S3D). Hence, we have successfully optimized a lysis-resealing method to study the RBC signaling pathways during merozoite invasion. We first evaluated the impact of preloading the different inhibitors into rRBCs on either cAMP levels or Ca^{2+} signaling using rRH5 protein. While a significant rise in cAMP level was observed in Empty rRBCs and HA-loaded rRBCs upon rRH5 binding at 2 min (Figure 3C), this can be drastically blocked by GPA, NF449 and 2′-*d*-3′-AMP which act before cAMP signaling (Figure 3C, bar chart in green), confirming that the binding of RH5 to basigin promotes host cAMP signaling. In contrast, no significant decrease in cAMP was seen with the impermeable inhibitors Rp-8-OH-cAMP, PKA (6–22) and N-methyl Vera which act downstream of cAMP signaling (Figure 3C, bar chart in red). Similarly, a sharp spike in detectable Ca^{2+} signals was captured in Fluo-4a.m. labeled rRBCs in the absence and presence of HA peptide upon rRH5 binding (Figure 3D), while the Ca^{2+} signals can be significantly blocked by the impermeable cAMP signaling and L-type Ca^{2+} channel inhibitors (Figure 3D). These results are consistent with our previous data using normal RBCs in this study, further confirming that RH5-basigin interaction induces the host cAMP signaling pathway to promote Ca^{2+} uptake from the extracellular space into the RBC cytosol through the host L-type Ca^{2+} channels. Our findings demonstrated a host cell derived signal cascade that connects RH5-bound basigin to the activation of RBC Ca^{2+} channels. Taken together, these data are consistent with the binding of parasite ligand to host receptor to promote Ca^{2+} influx through tightly regulated Ca^{2+} channels into the RBC via changes in RBC cAMP level during invasion.

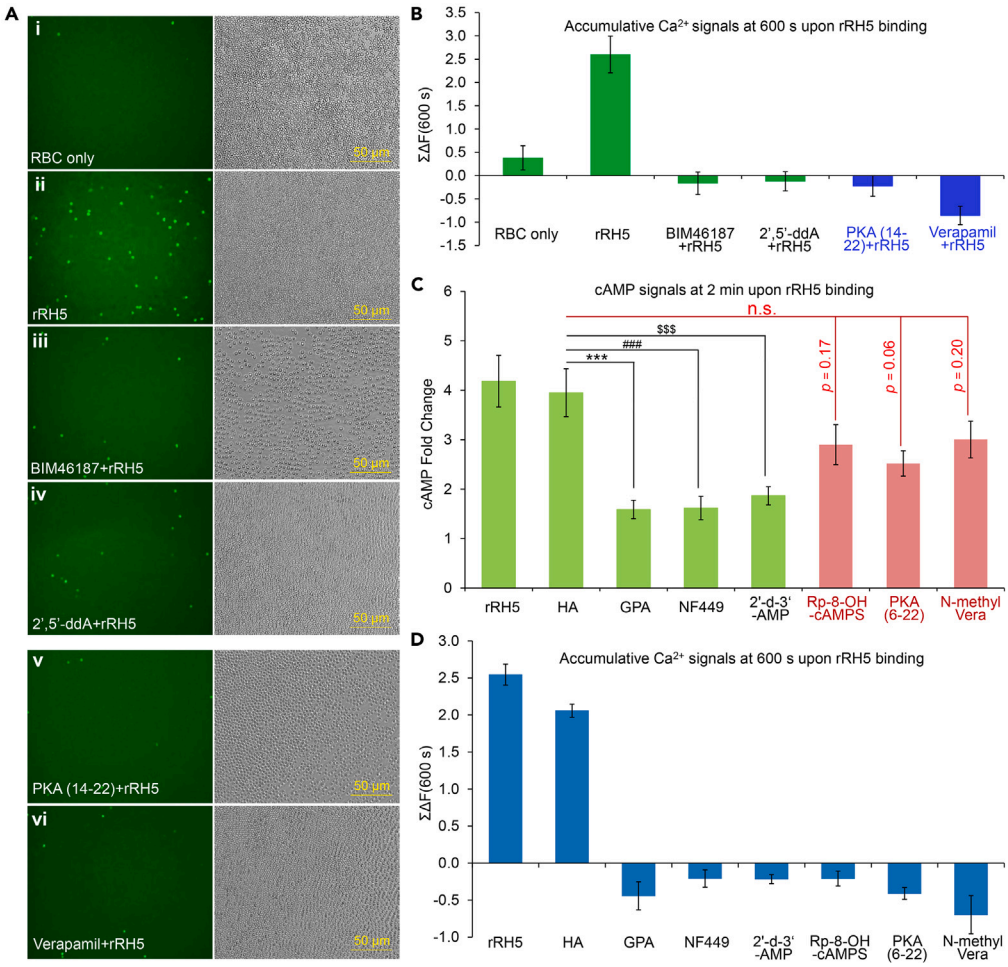

Figure 3. RH5-induced cAMP increase promotes RBC Ca^{2+} influx

Recombinant rRH5 was purified and used for all the assays.

(A) Fluorescence images of RBC Ca^{2+}. Fresh RBCs labeled with Fluo-4a.m. were incubated in the absence (i, RBC only) and presence of rRH5 (ii, rRH5) and presence of BIM46187 (iii, BIM46187+rRH5), 2′,5′-ddA (iv, 2′,5′-ddA + rRH5), PKA (14–22) (v, PKA (14–22)+rRH5) or verapamil (vi, Verapamil+rRH5) prior to rRH5 binding for 10 min. Fluorescence (left) and bright field (right) images were taken under 20× objective lens. Scale bar = 50 μm.

(B) RBC Ca^{2+} measurement by using fluorescence plate reader. The Ca^{2+} signal intensity of the samples obtained from (A) were also measured. Dynamics of RBC cytosolic Ca^{2+} level was measured over 600 s $\Sigma\Delta F(t)$ which reflects the cumulative change in RBC cytosolic Ca^{2+} was plotted as a bar chart. Experimental data presented as mean ± s.e.m, $n = 3$.

(C) cAMP inhibition immunoassay of resealed RBCs (rRBCs). To avoid the off-target effect on the permeable inhibitors mentioned above, membrane-impermeable inhibitors (Table 1) were loaded into rRBCs. The dynamics of rRBC cAMP level was measured upon rRH5 binding for 2 min in the absence (rRBC) and presence of impermeable inhibitors listed in Table 1. The cAMP reading in HA-loaded rRBCs was used as an internal positive control (HA). ***p = 0.01, ###p = 0.01 and $$$$p$ = 0.02 indicate the significant difference on fold change in rRBC cAMP level upon rHR5 binding in the presence of GPA, NF449 or 2′-*d*-3′-AMP compared to that in the HA-loaded rRBC, respectively (color in green). Whereas no significant inhibition effect was seen in Rp-8-OH-cAMPS, PKA (6–22) or N-methyl Vera with $p > 0.05$ including $p = 0.17$, $p = 0.06$ and $p = 0.20$ (color in red). Experimental data presented as mean ± s.e.m, $n = 3$.

(D) rRBC Ca^{2+} measurement by using fluorescence plate reader. Fluo-4a.m. labeled rRBCs were incubated with rRH5 protein in the absence (rRH5) and presence of impermeable inhibitors GPA, NF449, 2′-*d*-3′-AMP, Rp-8-OH-cAMPS, PKA (6–22) or N-methyl Vera, respectively. HA-loaded rRBC (HA) was used as an internal positive control. Dynamics of RBC cytosolic Ca^{2+} level was measured over 600 s $\Sigma\Delta F(t)$ which reflects the cumulative change in RBC cytosolic Ca^{2+} was plotted as a bar chart. Experimental data presented as mean ± s.e.m, $n = 3$. Statistical comparison was done using one-way ANOVA.

Activation of RBC cAMP signaling proteins and L-type Ca^{2+} channels directs junction formation

Our findings clearly showed that Ca^{2+} signaling in the RBC is mediated by host cAMP-dependent signaling upon RH5 binding and is consistent with live video microscopy demonstrating that host Ca^{2+} signaling is functionally conserved for merozoite invasion across *Plasmodium* species. However, whether the activation of pre-existing RBC L-type Ca^{2+} channels and cAMP signaling proteins are universally required for the invasion of mammalian RBCs across *Plasmodium* species remains unclear. To determine whether the roles of RBC cAMP signaling proteins and L-type Ca^{2+} channels are functionally conserved in *Plasmodium* invasion, we performed merozoite invasion inhibition assay of

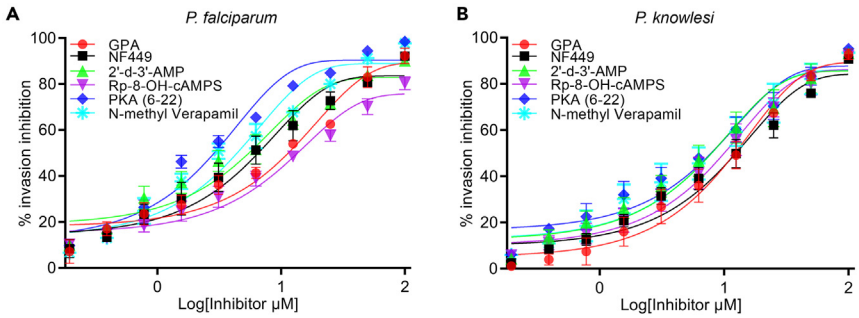

Figure 4. cAMP-Ca^{2+} signaling inhibitors block *P. falciparum* and *P. knowlesi* invasion

Merozoite invasion inhibition assays were performed using *P. falciparum* 3D7 (A) and *P. knowlesi* A1-H.1 (B) merozoites with human rRBCs that were preloaded with impermeable inhibitors listed in Table 1 at 2-fold increasing concentrations from 0.1953125 μM to 100 μM rRBCs preloaded with HA peptide were used as a positive control. % invasion inhibition of merozoites in the presence of inhibitors was compared with the invasion into rRBCs loaded with HA peptide. In a dose-response curve, the X values represent the logarithm of concentrations (μM) and the Yvalues represent % invasion inhibition. Experimental data were reported as mean ± s.e.m; $n = 3$.

P. falciparum and *P. knowlesi* in human rRBCs preloaded with impermeable inhibitors (Table 1). A dose-dependent invasion inhibition effect on both *P. falciparum* and *P. knowlesi* was seen in each inhibitor tested in both merozoites (Figure 4) as compared to HA-loaded rRBC control, indicating that cAMP signaling and L-type Ca^{2+} channels in the RBC are essential for invasion. In addition, we investigated whether the suppression of RBC Ca^{2+} signaling is a major cause of invasion inhibition. In line with previous observations, snapshots taken from live video microscopy of *P. falciparum* and *P. knowlesi* merozoite invasion in Fluo-4a.m. labeled human rRBCs in the absence (Figure 5Ai left panel, Video S5) and presence of HA peptide (Figures 5Aii and 5Bi left panels; Videos S6 and S13), exhibited successful invasions that begin with a Ca^{2+} influx inside the rRBC after merozoite initial attachment and reorientation, and the signal rapidly spread throughout the entire rRBC. These invaded rRBCs subsequently undergo massive deformation and Ca^{2+} decrease until the signal disappeared consistent with our previous data on normal RBCs.[11] Moreover, rRBC Ca^{2+} influx during the invasion process demonstrated a significant increase in fluorescence intensity when compared to uninfected rRBCs in the vicinity, as shown in right panel of Figures 5Ai, 5Aii, and 5Bi. To assess the impact of cAMP signaling protein inhibitors and L-type Ca^{2+} channel inhibitor on Ca^{2+} signaling in rRBCs during invasion, live video microscopy was also carried out by using preloaded rRBCs with each inhibitor. Interestingly, in all inhibitor-loaded rRBCs, Ca^{2+} influx was significantly blocked after the initial merozoite attachment (Figures 5Aiii, 5Aviii, 5Bii, 5Biii, and S4A–S4D; Videos S7, S8, S9, S10, S11, S12, S14, S15, S16, S17, S18, and S19), indicating that the cAMP signaling proteins and L-type Ca^{2+} channels are directly responsible for Ca^{2+} uptake into the RBC, which is required for both *P. falciparum* and *P. knowlesi* merozoite invasions.

To further evaluate the inhibitory effects of cAMP signaling protein inhibitors and L-type Ca^{2+} channel inhibitors on RBC Ca^{2+}, purified *P. falciparum* and *P. knowlesi* merozoites were incubated with rRBCs loaded with different inhibitors, and RBC Ca^{2+} signaling due to invasion was analyzed as described previously.[11,55] rRBCs in the absence and presence of HA peptide were used as positive controls. Merozoite invasion leads to a significant increase in detectable Ca^{2+} signals in positive controls, while the signals were drastically reduced in inhibitor-loaded rRBCs (Figure 5C), confirming that the cAMP signaling proteins and L-type Ca^{2+} channels play key roles in regulating RBC Ca^{2+} signaling during invasion. While *P. falciparum* and *P. knowlesi* merozoites do not utilize the same ligand-receptor binding on the RBC membrane, our data strongly imply the conserved involvement of an active cAMP-dependent signaling pathway induced by the binding of parasite ligand to host receptor triggers an increase of RBC cytosolic Ca^{2+} level to enable successful *Plasmodium* invasion. All these impermeable signaling inhibitors block merozoite invasion by preventing the RBC Ca^{2+} influx. However, our current understanding of the mechanistic implications on the merozoite itself from the initial attachment to entry into the RBC remains largely unexplored. It is known that the interruption of the complex containing apical membrane antigen 1 (AMA1) and rhoptry neck proteins (RONs) needed for tight junction formation does not affect RBC Ca^{2+} signaling and an RH5 monoclonal antibody is able to block a key step ahead of junction formation.[11,55] To assess whether the invasion inhibitory effect of these cAMP-Ca^{2+} signaling inhibitors takes place before or after junction formation, we performed merozoite junction blocking assays with rRBCs loaded with the different inhibitors as described previously.[55] Empty rRBCs and rRBCs loaded with HA were used as positive controls. Merozoites were arrested at the tight junction by treatment with cytochalasin D (Cyto D) and junction-arrested merozoites were counted. Strikingly, junction formation was significantly reduced ($p < 0.05$) whereby merozoites do not stay attached on the inhibitor-loaded rRBCs surface, compared to the positive controls of HA-loaded rRBCs (Figure 5D), further demonstrating that the inhibition effect of RBC cAMP-Ca^{2+} signaling crosstalk is acting at a step preceding junction formation.

Host cAMP/PKA-Ca^{2+} signaling cascade is manipulated by the parasite during invasion

The synergistic effect of cAMP and Ca^{2+} signaling is known to govern physiological functions in mammalian cells including RBCs and represents a crosstalk between two signaling pathways in which simultaneous stimulation of both signaling cascades induce a higher intensity of physiological responses than the predicted sum of intensities by the independent stimulation of each signaling cascade.[17,24,56,57] Yet little is known about the mechanisms by which both pathways interact in the RBC during merozoite invasion. Our current data indicates that the host

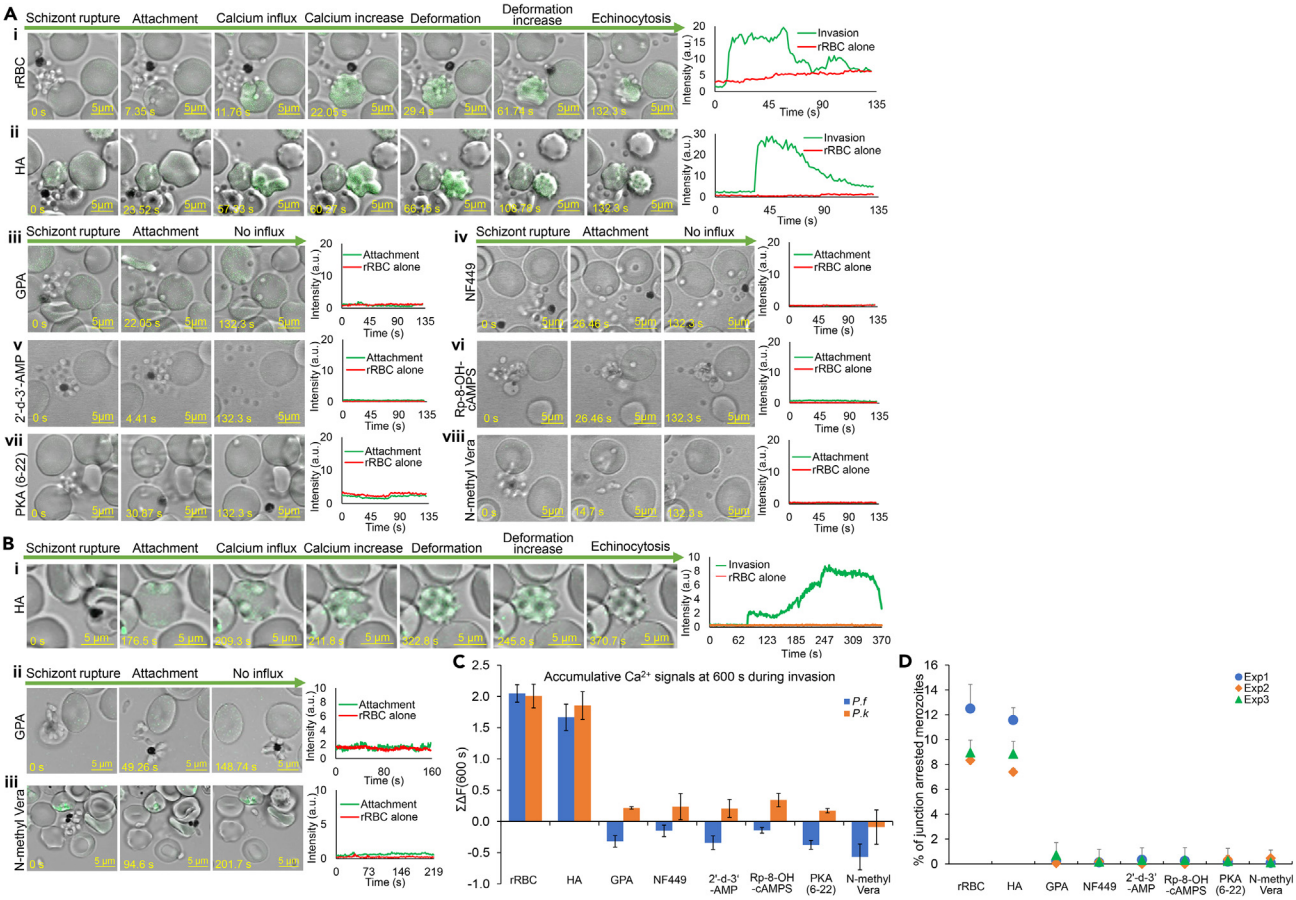

Figure 5. Live video microscopy of *P. falciparum* and *P. knowlesi* merozoite invasion

(A) Representative snapshots were taken from time-lapse live video microscopy of *P. falciparum* 3D7 merozoite invasion in the Fluo-4a.m. labeled human resealed RBCs in the absence (rRBC) (i) and presence of HA peptide (HA) (ii). Merozoite attaches to the RBC after the schizont rupture and reorients followed by Ca^{2+} influx that spreads throughout the entire resealed RBC. The Ca^{2+} influx causes a massive deformation, and the signal starts to decrease when echinocytosis happens (Videos S5 and S6). Representative video snapshots were also taken for both 3D7 invasion in the Fluo-4a.m. labeled rRBCs in the presence of (iii) GPA, (iv) NF449, (v) 2′-*d*-3′-AMP, (vi) Rp-8-OH-cAMPS, (vii) PKA (6–22) and (viii) N-methyl Vera (Videos S7–S12).

(B) Snapshots of *P. knowlesi* A1-H.1 merozoite invasion in the Fluo-4a.m. labeled human resealed RBCs in the presence of HA peptide (i), GPA (ii) and N-methyl Vera (iii). Merozoite attaches to the rRBC loaded with HA peptide (i) after the schizont rupture and reorients followed by Ca^{2+} influx that spreads throughout the entire resealed RBC. The Ca^{2+} influx causes a massive deformation, and the signal starts to decrease when echinocytosis happens (Video S13). In snapshots of (A-iii-viii) and (B-ii-iii), the merozoite released from a mature schizont attaches and apically reorients, but it is unable to penetrate the RBC with no Ca^{2+} influx (Videos S14 and S19). Dynamics of rRBC Ca^{2+} signals was measured. Ca^{2+} fluorescence intensity was indicated next to each of the snapshot. Relative time was shown in seconds. Scale bar = 5 μm.

(C) rRBC Ca^{2+} measurement by using fluorescence plate reader during *P. falciparum* and *P. knowlesi* invasion. Fluo-4a.m. labeled rRBCs were incubated with 3D7 (*P.f*) and A1-H.1 (*P.k*) merozoites in the absence (rRBC) and presence of inhibitors GPA, NF449, 2′-*d*-3′-AMP, Rp-8-OH-cAMPS, PKA (6–22) or N-methyl Vera, respectively. HA-loaded resealed RBC (HA) was used as an internal positive control. Dynamics of RBC cytosolic Ca^{2+} level was measured over 600 s $\Sigma\Delta F(t)$ which reflects the cumulative change in RBC cytosolic Ca^{2+} was plotted as a bar chart. Experimental data presented as mean ± s.e.m, $n = 3$.

(D) cAMP and Ca^{2+} signaling inhibitors impede junction formation. 3D7 schizonts were incubated with rRBC in the absence and presence of inhibitors (Table 1) under Cyto D treatment. HA-loaded rRBCs were used as an internal control. Junction-arrested merozoites were counted microscopically. % junction-arrested merozoites of tested samples from 3 biological replicates were plotted. All inhibitors effectively blocked junction formation. Experimental data presented as mean ± s.e.m, $n = 3$.

cAMP signaling proteins and L-type Ca^{2+} channels are individually key players of RBC Ca^{2+} influx during invasion. As Ca^{2+} uptake from an extracellular environment into the RBC is potentially driven by the activation of Ca^{2+} voltage-gated channels, we aim to determine whether a crosstalk between the cAMP and Ca^{2+} signaling pathways influences the entry of extracellular Ca^{2+} signals via the L-type Ca^{2+} channels during invasion. We performed a checkerboard invasion inhibition assay to measure the combined inhibition level of rRBCs loaded with dual combinations of impermeable signaling inhibitors. The impermeable L-type Ca^{2+} channel inhibitor N-methyl verapamil was selected as the reference inhibitor to be paired with GPA, NF449, 2′-*d*-3′-AMP, Rp-8-OH-cAMP, or PKA (6–22), respectively. All dual inhibitor combinations exhibited drastically higher invasion inhibition levels when compared to that of individual inhibitor (Figure 6A). This is evident when

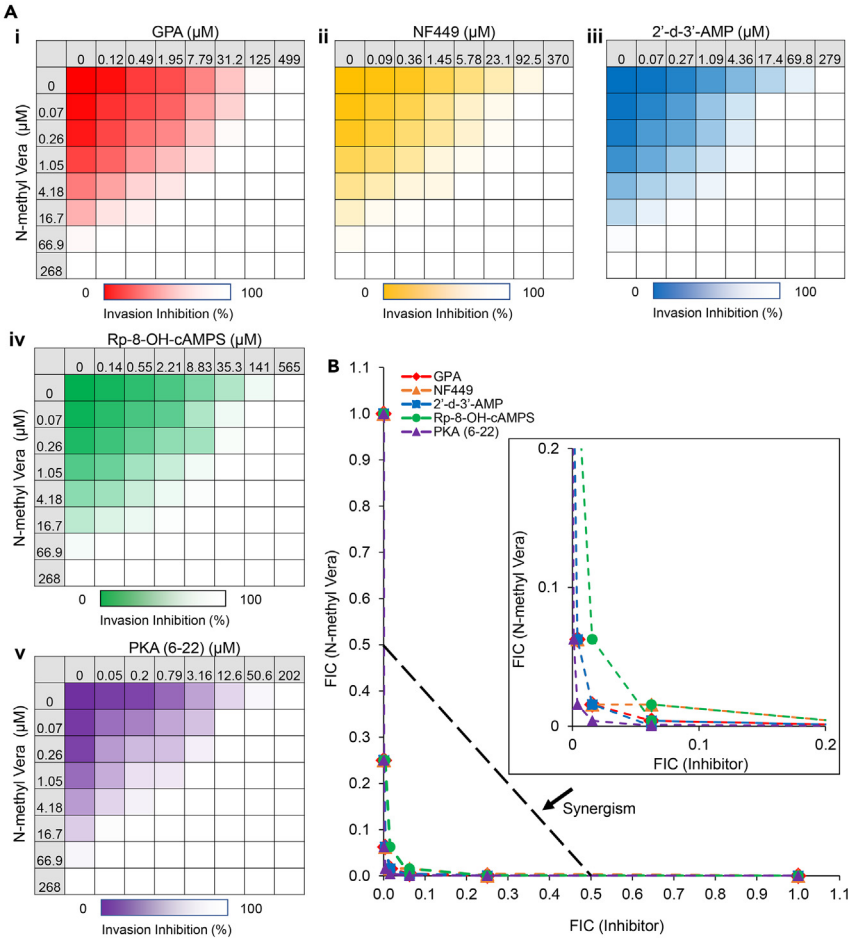

Figure 6. Synergistic effect of cAMP-Ca^{2+} signaling inhibitors block junction formation during merozoite invasion

(A) Inhibition heat plots of 3D7 merozoite invasion into rRBCs. Resealed RBCs were pre-loaded with dual combinations of Ca^{2+} channel blocker (N-methyl Vera) and other cAMP signaling inhibitors including GPA (i, red), NF449 (ii, yellow), 2′-*d*-3′-AMP (iii, blue), Rp-8-OH-cAMPS (iv, green), and PKA (6–22) (v, purple). All inhibitors were loaded in rRBCs at about 4-fold increasing concentrations including N-methyl Vera shown in each table vertically, while the other inhibitors shown horizontally in color matrices. Colors in the dose-response matrices from the darkest to white indicate different levels of invasion inhibitions from 0% to 100% obtained from Figure S3.

(B) Isobologram plot of five different checkerboard invasion inhibition data from Figure S4. The range of Fractional Inhibitory Concentration (FIC) values surrounding the black dotted line with arrow in black from 0 to 0.5 represents a synergistic isobole. Data points below this line indicate potent synergism, while the data points above this line indicate partial synergism. Inset: zoomed plot at 0.15 of both x and y axis for better visualisation.

the inhibitor concentrations were increased, the invasion inhibition level of paired checkerboard squares peaked higher than the expected sum of individual inhibition levels by both inhibitors (Figures 6A and S5), suggesting a synergistic relationship between the host cAMP and Ca^{2+} signaling pathways that is functionally active in merozoite invasion. Furthermore, an isobologram of all five checkerboard invasion inhibition assays was applied between N-methyl verapamil and its paired cAMP signaling inhibitors. Since the Fractional Inhibitory Concentration (FIC) index <0.5 indicates a synergistic inhibitory interaction,[58,59] our isobolographic analysis revealed potent synergism in invasion inhibition by N-methyl verapamil and its paired cAMP signaling inhibitor in all five dual inhibitor combinations (Figure 6B), confirming that a host-specific crosstalk exists between the cAMP and Ca^{2+} signaling pathways during invasion.

Taken together, our work showed that the RBC cAMP signaling proteins and L-type Ca^{2+} channels are operating synergistically in a functionally conserved cAMP-Ca^{2+}-mediated signaling cascade that regulates RBC Ca^{2+} influx from the extracellular space into the RBC cytosol during invasion across *Plasmodium* species. In addition, we provided strong evidence on the functional role of a host cAMP-Ca^{2+} signaling crosstalk that governs junction formation necessary for successful merozoite invasion.

RH5-basigin binding forms a multimeric RBC membrane complex containing β2-adrenergic receptor

Nine proteins from the *P. falciparum* RH and EBL families, such as RH1, RH2a, RH2b, RH4, RH5, EBA175, EBA181, EBA140, EBL-1, bind to RBC surface receptors to facilitate the invasion process.[60,61] Basigin is the specific host receptor of *P. falciparum* ligand RH5, and this interaction is

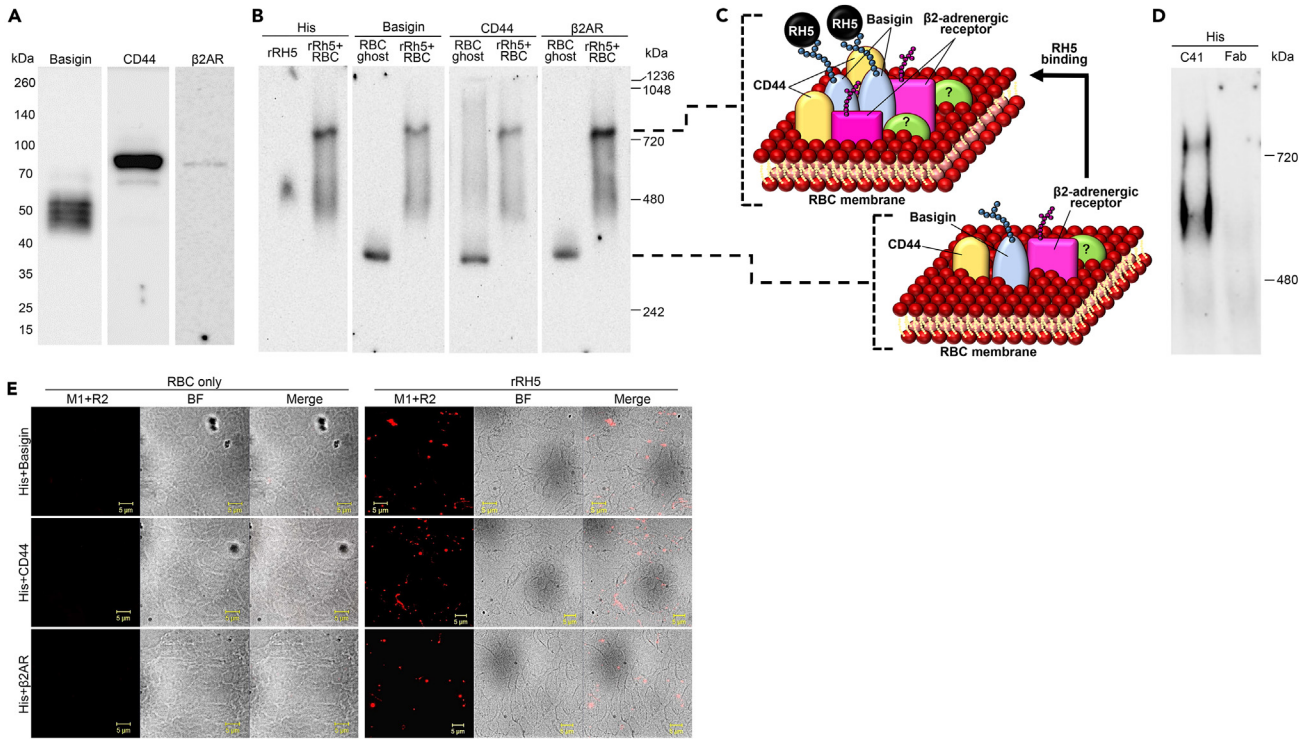

Figure 7. Basigin associates with membrane proteins to form a multimeric complex on the RBC membrane

(A) Unbound RBC ghosts were separated on a single 10% SDS-PAGE and probed with basigin, CD44 and β2AR antibodies.

(B) Basigin is part of RBC membrane complex containing CD44 and β2AR. Unbound RBC ghosts (RBC ghost) and eluted samples of RH5-bound RBC ghosts (rRH5+RBC) were separated on a single 5% Native-PAGE and probed with basigin, CD44 and β2AR antibodies. Anti-His antibody (His) was also used to detect rRH5 itself (rRH5) and RH5-bound RBC ghosts (rRH5+RBC). The protein molecular weight (kDa) is indicated on either the left or right side.

(C) Schematic model of basigin-associated complex derived from (B) containing CD44 and β2AR on the RBC membrane upon RH5 binding. RH5-bound basigin dimerization leads to increased organisation and recruitment of RBC proteins (top panel) in a pre-existing multimeric complex consisting of CD44, β2AR and other unknown membrane proteins (bottom panel). "?" represents unknown RBC proteins.

(D) RH5-associated complex is abolished by anti-basigin Fab fragment. rRH5 was incubated with RBCs in the presence of RH1 mAb C41 (C41) or anti-basigin Fab fragment (Fab), respectively. Eluted samples of RH5-bound RBC ghosts were separated on a single 5% Native-PAGE and probed with anti-His antibody (His). The protein molecular weight (kDa) is indicated on either the left or right side.

(E) RH5-basigin associated complex by Proximity Ligation Assay (PLA). The blood smears of RBC only (RBC only, left panel) and RH5-bound RBC (rRH5, right panel) were dually probed with α-His and α-basigin (His+Basigin), α-His and α-CD44 (His+CD44) and α-His and α-β2AR (His+β2AR), respectively. The slides were then probed with corresponding secondary antibodies conjugated with either plus or minus PLA probes. Fluorescent images (M1+R2), bright field images (BF) and merged images (Merge) are shown. The interaction between rRH5 and basigin or CD44 or β2AR was observed as red dots. Scale bars = 5 μm.

essential for invasion.[62] In *P. knowlesi*, the binding of *P. knowlesi* Duffy binding protein α (PkDBPα) to host Duffy antigen/receptor for chemokines (DARC) is required for invasion into human and macaque RBCs.[63] Despite exhibiting species-specific differences, the importance of ligand-receptor binding on the RBC membrane indicate that these interactions could lead to a conserved activation of innate RBC cAMP-Ca^{2+}-dependent signaling pathways necessary for invasion. In *P. falciparum* invasion, RH5-basigin interaction triggers RBC Ca^{2+} influx from the extracellular environment that leads to RBC cytoskeleton changes[11,29] in line with our data on the parasite exploiting the host cAMP-Ca^{2+} signaling crosstalk to direct junction formation, while at the same time it is clear that the cytoplasmic tail of basigin does not perform a functional role in invasion.[64] Therefore, the question on how the binding of RH5 to basigin triggers cAMP-Ca^{2+} signaling in RBCs during invasion still needs to be resolved. It has been shown that the RBC utilizes its own cAMP and Ca^{2+} signaling pathways to enable Ca^{2+} influx which regulates membrane deformability.[24] Interestingly, basigin associates with β2AR in a pre-existing complex on the endothelial cell membrane which reinforces bacterial adhesion during meningococcal invasion.[65] Moreover, the functional interaction between basigin and CD44 on the membrane during invasion suggests that CD44 is a binding partner of RH5-bound basigin.[66] Taken together, this implies that RH5-bound basigin interacts with neighboring membrane proteins in a chain of protein-protein stimulations that in turn relay signals from an extracellular to intracellular environment to promote downstream invasion events. To first detect the presence of basigin, CD44 and β2AR on the RBC membrane, we extracted RBC ghosts and performed SDS-PAGE and western blot followed by probing with α-basigin, α-β2AR and α-CD44 antibodies. All three Abs recognize their expected proteins in size respectively (Figure 7A), confirming the specificity of the antibodies and the presence of basigin, CD44 and β2AR on the RBC surface. To address whether RH5-basigin binding forms a complex with CD44 and β2AR, we extracted RBC ghosts in the absence and presence of functional rRH5 and carried out Native-PAGE and western

blot. A band at approximately 300–400 kDa in size was recognized by α-basigin, α-CD44 and α-β2AR Abs in the RBC ghost extraction, respectively (Figure 7B), indicating a pre-existing basigin-associated complex is formed on the RBC membrane. Strikingly, all three antibodies detected a large increase in protein complex size to approximately 800 kDa upon rRH5 binding (Figure 7B), demonstrating that RH5-basigin dimerization leads to an increased assembly and organization of diverse RBC membrane proteins including CD44 and β2AR (Figure 7C). α-His antibody was used as a loading control of rRH5 and confirmed the presence of rRH5 in the extraction. To further confirm the specificity of RH5 binding to the basigin-associated complex, we also carried out rRH5 pull-down of RBC ghosts in the presence of anti-basigin Fab fragment or RH1 inhibitory mAb C41.[11,55,67] Fab abolished the formation of the multimeric RH5-basigin complex, whereas C41 did not prevent the RH5-basigin complex formation, indicating that Fab selectively blocks RH5-basigin interaction and RH5 binding is specific in all the pull-down experiments (Figure 7D). To further determine whether indeed RH5 is in close proximity with basigin, CD44 and β2AR on the surface of the RBC membrane, we performed the proximity ligation assay (PLA) between RH5 and these three RBC membrane proteins. We observed that RH5 closely associates with basigin, CD44 and β2AR in RH5-bound RBCs with multiple cells exhibiting red fluorescence signals, while there was no signal detected in the absence of RH5 (Figure 7E). To confirm the specificity of the PLA, we evaluated whether DARC, an RBC membrane protein not expected to be part of this complex, interacts with RH5 bound to the RBC. Fluorescent labeled RBCs probed with α-DARC verify the specificity of the antibody as well as the presence of DARC on the RBC surface (Figure S6A). No fluorescence signal was observed when evaluating the proximity between RH5 and DARC (Figure S6B), supporting that DARC is not associated with RBC membrane-bound RH5. In line with our previous work, RH5 inhibitory mAb RH5(7)[11] blocks RH5-basigin binding and leads to the absence of PLA signals (Figure S6C), further confirming that RH5 is associated with RBC membrane-bound invasion complex. Overall, the presence of the cAMP-inducing β2AR in a multimeric RBC invasion complex suggests that the binding of species-specific parasite ligand to RBC surface receptor initiates an activation cascade of membrane proteins that triggers host cAMP-dependent signaling pathways to facilitate Ca^{2+} influx in the RBC.

DISCUSSION

cAMP was the first second messenger described[68] and cAMP-mediated signaling pathways regulate a broad range of important biological processes under both physiological and pathological conditions. *Plasmodium* parasites also utilize cAMP-Ca^{2+} signaling, which are crucial for invasion, and blocking them impedes host cell invasion.[28,69–71] cAMP signaling not only plays a critical role in nucleated cell such as the brain, liver and kidney cells,[72] but also in RBCs that lack many subcellular organelles and compartments such as nuclei and mitochondria.[15] Despite these structural deprivations, RBCs retain multiple signaling pathways to regulate reversible morphological changes in response to extracellular signaling conditions.[13,14] Moreover, the synergistic interaction between cAMP and Ca^{2+} signaling is known to regulate feedback signaling loops and potentiate biochemical responses in mammalian cells including RBCs.[17,24,73] Studies have shown that cAMP-PKA and Ca^{2+} signaling controls RBC deformation and aggregation in response to mechanical and microrheological changes.[15,36] Yet how *Plasmodium* parasites manipulate host cell signaling nor whether RBC cAMP-Ca^{2+} signaling pathway plays any crucial roles during invasion has not been well-elucidated.

Plasmodium parasite is the causative agent of the malaria disease in mammalian hosts including humans, non-human primates (NHP) and rodents, and are primarily transmitted by *Anopheles* mosquitoes. More than 30 species of *Plasmodium* have been reported in NHPs and are generally restricted to the invasion of phylogenetically related hosts.[74] However, certain NHPs share *Plasmodium* parasites with humans and this raises the question whether parasite host-switching is driven by ongoing ecological and evolutionary mechanisms which enables infection in NHPs and humans.[75–77] The recent emergence of cross-species malaria transmission in Malaysia poses a serious health risk as highlighted by the capability of zoonotic *P. knowlesi* merozoites to invade both macaque and human RBCs.[6,77] The invasion preference of different *Plasmodium* species for specific hosts and ability to develop in RBCs have been attributed to the unique genomic repertoire of multigene families in species which determines their host cell selection and host-switching capability.[76,78] *Plasmodium* merozoites possess a wide range of proteins in their secretory organelles and surface that are essential for invasion, notably the binding of ligands to receptors and the establishment of the tight junction.[4,6,79–82] A subset of these proteins belongs to two major protein families, the EBLs and RHs, which universally function as RBC adhesion ligands across *Plasmodium* species to facilitate successful entry of the merozoite into the RBC.[27] Previous studies from our group have shown that RH1 and RH2b trigger merozoite Ca^{2+} signaling during invasion, which can be blocked with mAbs targeting either one.[55,83] However, only RH5 on its own can trigger RBC Ca^{2+} signaling.[11] mAbs against RH5 but not RH1 inhibit invasion by blocking RBC Ca^{2+} signaling but not merozoite Ca^{2+} signaling during invasion. Studies have shown that *P. knowlesi* possess two types of RH family normocyte-binding proteins PkNBPXa and PkNBPXb to bind to macaque RBCs, whereas PkNBPXa is the only ligand required for human RBC invasion.[6] RH5-basigin interaction was first identified to be able to trigger RBC Ca^{2+} signaling that leads to host cell cytoskeletal remodeling,[11] suggesting that the RBC, which was once thought to be passive, plays a key role in facilitating the invasion process. Proteomic analysis of RBCs from humans, macaques, and mice demonstrates that various membrane and soluble protein orthologs likely share functions across RBC species and RBC cytoskeleton protein isoforms in all three species exhibit overall similarity in the cytoskeletal network.[84] Our data in turn implies that there are conserved host cell signaling pathways downstream of the invasion ligand binding. As the binding of a parasite ligand to host receptor is sufficient to induce RBC Ca^{2+} signaling derived from extracellular Ca^{2+} uptake, this also infers that the parasite has manipulated one or more host cell signaling pathways downstream of the binding. Indeed, our study here reveals further insights into a functionally conserved host RBC cAMP-Ca^{2+} signaling cascade essential for *Plasmodium* invasion. Overall, our work highlights that the host cell cAMP signaling pathway links species-specific ligand-receptor binding to voltage-gated Ca^{2+} channels including L-type Ca^{2+} channel activation on the RBC membrane during *Plasmodium* invasion. While there has been mounting evidence of PKA phosphorylation sites on the α and

β subunits of L-type Ca^{2+} channels that increase channel activities,[18,19,85–87] whether RBC L-type Ca^{2+} channels can be activated directly or indirectly by the cAMP-mediated release of PKA catalytic subunits during invasion needs to be further investigated. Taken together, these data suggest that Ca^{2+} signaling in both merozoite and its host RBC are equally important for invasion and the RBC is not just a passive bystander in invasion. It is though clear that in both *P. falciparum* and *P. knowlesi* invasion, the activation of cAMP signaling proteins plays an upstream regulatory role in triggering extracellular Ca^{2+} uptake via activated L-type Ca^{2+} channels and the perturbation of these host protein activities effectively blocks this Ca^{2+} influx, and ultimately, merozoite invasion.

Basigin is a commonly expressed membrane protein that is involved in a variety of physiological and pathological activities of mammalian cells[88–91] and its interaction with RH5 is essential for *P. falciparum* invasion.[62] Basigin has been recently reported to be a receptor of the spike protein that undergoes a novel route for SARS-CoV-2 infection into host cells, highlighting a promising target for COVID-19 antiviral drug development,[92] but little is known about its exact molecular functions on the RBC surface during merozoite invasion. Interestingly, basigin on the mouse RBC surface has been identified to be the putative *P. yoelii* EBL receptor, suggesting that the binding to basigin is required for multiple *Plasmodium* invasions.[10] Our data demonstrate that basigin forms a pre-existing membrane complex with CD44 and β2AR prior to invasion which potentially recruit additional RBC membrane proteins to tightly associate with RH5-bound basigin in invasion, indicating that the increased protein assembly and organisation on the RBC membrane upon RH5-basigin binding is critical in driving downstream invasion events. This is consistent with the functional interaction between basigin and β2AR that mediates the activation of canonical signaling pathways including cAMP, in a membrane complex to initiate host cell signaling events.[65] This is also in line with β2AR agonists stimulating cAMP production by AC in RBCs to lead to increased *P. falciparum* infection that can be perturbed by β2AR antagonists and Gα inhibitory peptides,[53,93] further highlighting that β2AR-activated cAMP signaling is critical for invasion. Interestingly, Satchwell et al. has established a tractable system for genetic manipulation of the BEL-A cell line to explore host receptor requirements for *P. falciparum* invasion. Modified BEL-A reticulocytes expressing the truncated basigin protein by a deletion of its C-terminal cytoplasmic domain exhibit similar invasive susceptibility to that of unmodified BEL-A-derived reticulocytes, indicating that C-terminal of basigin is not essential for invasion.[64] With reference to our data, these studies signify that RH5-bound basigin does not directly activate β2AR on the RBC membrane but assembles with β2AR in a multimeric protein complex to modulate the host intracellular cAMP dynamics and in turn trigger a cAMP-mediated signaling cascade. Our study also provides a mechanistic insight into the role of the host cAMP-Ca^{2+} signaling crosstalk in merozoite invasion, in which both signaling pathways direct changes on the RBC that are important for the proper insertion and anchoring of parasite AMA1 and RON proteins which are key players of junction formation. Merozoite junction formation can be completely abolished once the βAR-cAMP-PKA signaling pathway and Ca^{2+} channels are blocked by their specific inhibitors. This thereby establishes a functional relationship between merozoite invasion and previous studies showing the RH5-triggered RBC Ca^{2+} signaling promotes phosphorylation of specific RBC cytoskeleton proteins and overall alterations in RBC cytoskeleton architecture. Further investigations are now required to characterize the member proteins of the RBC invasion complex and to elucidate the mechanistic events in junction formation and RBC cytoskeleton changes that are governed by the host cAMP-Ca^{2+} signaling crosstalk.

Taken together, we have successfully dissected the host cell signaling cascade that is activated by the binding of parasite ligand to host receptor and how the host signaling proteins can be targeted to block merozoite invasion. We hypothesise that upon parasite ligand binding on the RBC surface, a pre-existing RBC invasion membrane complex undergoes increased protein association that subsequently activates the β-adrenergic receptor (Figure 8A-I). The activation of β-adrenergic receptor via Gαs in turn triggers the host cAMP-PKA signaling pathway by converting ATP to cAMP through AC via a 3′-5′-ATP-cyclization reaction (Figures 8A-II-IV). PKA either directly or indirectly activate the Ca^{2+} channels to enable Ca^{2+} influx in the RBC required for merozoite invasion (Figure 8A-V-VI). The activation of PKA also phosphorylates RBC cytoskeleton proteins, such as adducin and protein 4.1R, thereby destabilising the cytoskeletal network and loosening the RBC membrane to direct junction formation and in turn enable parasite entry (Figure 8A-V-VII–8C). Our data clearly demonstrated that the signaling pathways in both merozoite and the host RBC run concurrently and independently from each other during invasion. Understanding host cAMP and Ca^{2+} signaling events that contribute to *Plasmodium* merozoite invasion can therefore open avenues for alternative drug intervention strategies. Our current findings have made a significant step forward in determining the synergistic effects of merozoite-induced cAMP-Ca^{2+} signaling crosstalk in the RBC and provided solid evidence of how the parasite is able to manipulate host cell signaling cascades to facilitate successful merozoite invasion.

Limitations of the study

The study relies on the use of several inhibitors that target specific known signaling molecules. While significant efforts have been made to rule out nonspecific cross reactivity to other proteins there remains a possibility, however unlikely, that the inhibition of invasion observed could be caused by some off-target interaction. An additional caveat is that at this stage it unlikely that the work identified all the components of the RBC cAMP-Ca^{2+} signaling pathway in *Plasmodium* parasite invasion, particularly in relation to the complete RBC membrane proteins of the invasion complex. This is due to the difficulty to genetically manipulate the RBC as well as generating sufficient amounts of RH5-bound RBC ghosts for large-scale protein screening methods such as mass spectrometry.

RESOURCE AVAILABILITY

Lead contact

Further information and requests should be directed to the Lead contact, P.R.P. (prpreiser@ntu.edu.sg).

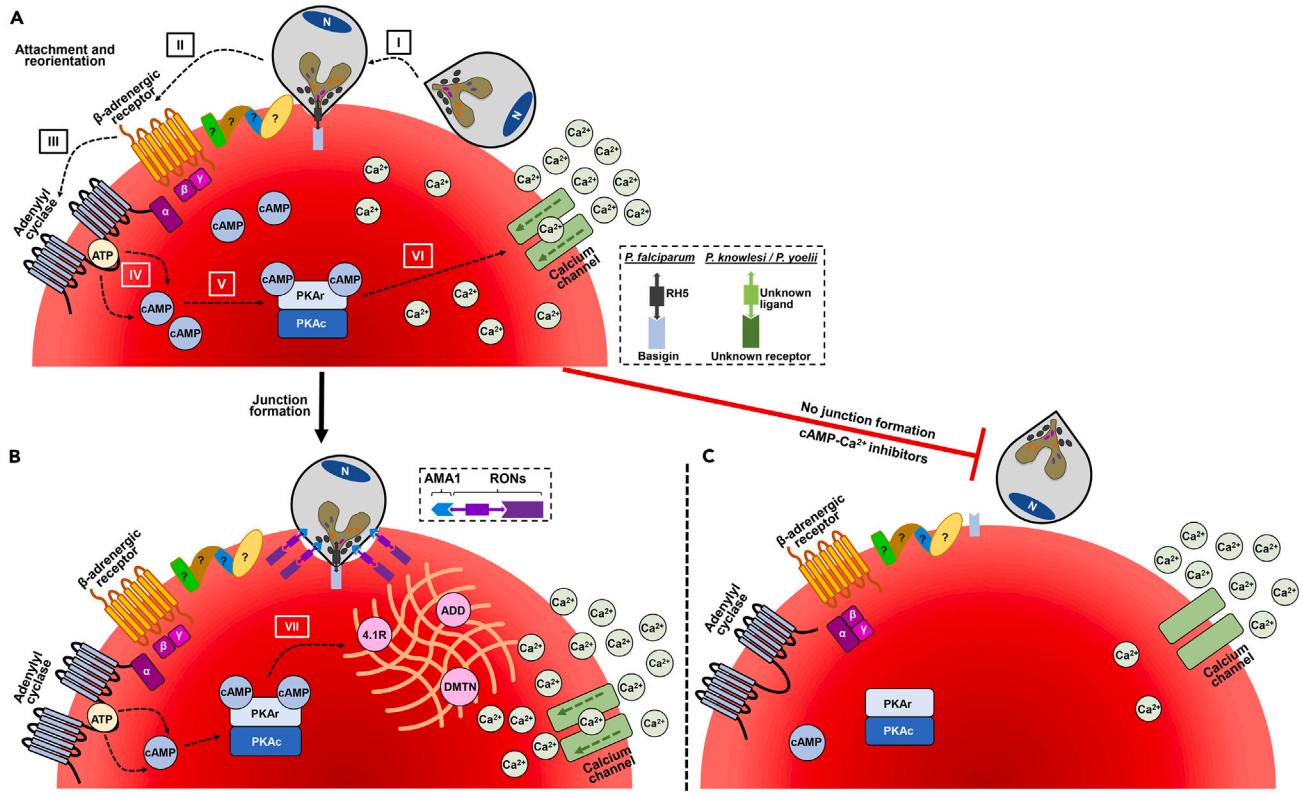

Figure 8. Schematic model of RBC cAMP-Ca^{2+} signaling during merozoite invasion

A functionally conserved RBC cAMP-Ca^{2+} signaling crosstalk is manipulated by *Plasmodium* parasites to facilitate successful invasion.

(A) Upon the merozoite release, it attaches and reorients its apical end toward the RBC membrane (I). The binding of species-specific parasite ligands including RH5 in *P. falciparum* and unknown ligands in *P. knowlesi* and *P. yoelii* to their respective host receptors (indicated in right panel) triggers an activation cascade of neighboring RBC molecules in a multimeric membrane complex which contains and activates the β-adrenergic receptors (II). Activation of βAR triggers the dissociation of stimulatory G protein alpha (Gαs) from heterotrimeric G proteins (αβγ subunits) that binds to the transmembrane adenylyl cyclase (III). Activation of transmembrane adenylyl cyclase generates cAMP from ATP via 3′-5′-ATP-cyclization reaction (IV). cAMP molecules bind to the PKA (V) and subsequently activates the kinase. PKA may directly or indirectly be involved in the activation of L-type Ca^{2+} channels (VI).

(B) PKA may phosphorylate the cytoskeleton proteins to promote overall changes of RBC cytoskeleton structure (VII) which is involved in the insertion of the AMA1-RONs complex (indicated in the rectangle) required for junction formation.

(C) Perturbation of the RBC cAMP-Ca^{2+} signaling cascade by inhibitors blocks junction formation. "?" represents the unknown RBC membrane proteins. "N" represents nuclei in blue.

Materials availability

Request for plasmids, antibodies or resources used/generated in this study should be directed to the lead contact, P.R.P. (prpreiser@ntu.edu.sg).

Data and code availability

All data reported in this paper after it is published will be shared by the lead contact upon request. This paper does not report original code. Any additional information required to reanalyze the data reported in this paper is available from the lead contact upon request.

ACKNOWLEDGMENTS

We are grateful to all the human blood donors. We are grateful to Assoc. Prof. Pablo Bifani and Ms. Lai Si Qi from National University of Singapore and Dr. Adeline Chua from A*STAR Infectious Diseases Labs, Singapore for the monkey blood collections. We also thank the NTU Protein Production Platform for expression and purification of recombinant RH5 and Pink Flamindo proteins. This research is supported by Singapore Ministry of Education Academic Research Fund Tier 2 (MOE2017-T2-1-034, MOE-T2EP30121-0013 and MOE2019-T3-1-007). The funders had no role in study design, data collection and analysis, decision to publish, or preparation of the manuscript.

AUTHOR CONTRIBUTIONS

J.J.M.Y. and X.G. contributed extensively and equally to the experiments, analyzed the data and wrote the manuscript. J.J.M.Y., X.G., P.P., and P.R.P. conceived the experiments. J.W.A. maintained *P. knowlesi* A1-H.1 and *P. yoelii* YM cultures as well as extracted schizonts for the study. M.W.C., J.J.L.N., and L.J. performed the recombinant RH5 protein expression and purification. J.J.M.Y., X.G., S.K.L., and H.Y.L. performed the live video microscopy and analyzed the data. P.R.P. supervised the project, analyzed the data, and wrote the manuscript.

DECLARATION OF INTERESTS

The authors declare no conflict of interest.

STAR★METHODS

Detailed methods are provided in the online version of this paper and include the following:

- KEY RESOURCES TABLE
- EXPERIMENTAL MODEL AND STUDY PARTICIPANT DETAILS
  - Human subjects
  - Animal subjects
  - Parasite culture and isolation of schizonts and/or merozoites
- METHOD DETAILS
  - Generation and purification of recombinant RH5 protein
  - Erythrocyte binding assay
  - Generation of RBC ghosts
  - Western blot analysis of RBC ghosts
  - Proximity ligation assay (PLA)
  - Immunofluorescence assay and microscopy
  - Generation of resealed RBC with membrane-impermeable signaling inhibitors
  - cAMP immunoassay
  - Dot blot analysis of resealed RBCs
  - Generation of Pink Flamindo protein
  - Viability assay of free merozoites
  - Merozoite invasion inhibition assay with EGTA
  - Merozoite invasion inhibition assay with membrane-impermeable inhibitors
  - Visualisation and measurement of RBC cAMP or Ca^{2+} by fluorescent microscopy and fluorescence plate reader
  - Live video microscopy
  - Checkerboard invasion inhibition assay
  - Junction-arrested merozoite blocking assay
- QUANTIFICATION AND STATISTICAL ANALYSIS

SUPPLEMENTAL INFORMATION

Supplemental information can be found online at https://doi.org/10.1016/j.isci.2024.111052.

Received: March 7, 2023
Revised: June 20, 2024
Accepted: September 24, 2024
Published: September 26, 2024

REFERENCES

1. World Health Organization (2021). World Malaria Report 2021 (World Health Organ), p. 263.
2. Gunalan, K., Gao, X., Yap, S.S.L., Huang, X., and Preiser, P.R. (2013). The role of the reticulocyte-binding-like protein homologues of Plasmodium in erythrocyte sensing and invasion. Cell Microbiol. *15*, 35–44.
3. Iyer, J.K., Amaladoss, A., Genesan, S., and Preiser, P.R. (2007). Variable expression of the 235 kDa rhoptry protein of Plasmodium yoelii mediate host cell adaptation and immune evasion. Mol. Microbiol. *65*, 333–346.
4. Jaskiewicz, E., Jodłowska, M., Kaczmarek, R., and Zerka, A. (2019). Erythrocyte glycophorins as receptors for Plasmodium merozoites. Parasites Vectors *12*, 317.
5. Lopaticki, S., Maier, A.G., Thompson, J., Wilson, D.W., Tham, W.H., Triglia, T., Gout, A., Speed, T.P., Beeson, J.G., Healer, J., and Cowman, A.F. (2011). Reticulocyte and erythrocyte binding-like proteins function cooperatively in invasion of human erythrocytes by malaria parasites. Infect. Immun. *79*, 1107–1117.
6. Moon, R.W., Sharaf, H., Hastings, C.H., Ho, Y.S., Nair, M.B., Rchiad, Z., Knuepfer, E., Ramaprasad, A., Mohring, F., Amir, A., et al. (2016). Normocyte-binding protein required for human erythrocyte invasion by the zoonotic malaria parasite Plasmodium knowlesi. Proc. Natl. Acad. Sci. USA *113*, 7231–7236.
7. Muh, F., Lee, S.K., Hoque, M.R., Han, J.H., Park, J.H., Firdaus, E.R., Moon, R.W., Lau, Y.L., and Han, E.T. (2018). In vitro invasion inhibition assay using antibodies against Plasmodium knowlesi Duffy binding protein alpha and apical membrane antigen protein 1 in human erythrocyte-adapted P. knowlesi A1-H.1 strain. Malar. J. *17*, 272.
8. Williams, A.R., Douglas, A.D., Miura, K., Illingworth, J.J., Choudhary, P., Murungi, L.M., Furze, J.M., Diouf, A., Miotto, O., Crosnier, C., et al. (2012). Enhancing blockade of Plasmodium falciparum erythrocyte invasion: assessing combinations of antibodies against PfRH5 and other merozoite antigens. PLoS Pathog. *8*, e1002991.
9. Wright, G.J., and Rayner, J.C. (2014). Plasmodium falciparum erythrocyte invasion: combining function with immune evasion. PLoS Pathog. *10*, e1003943.
10. Yuguchi, T., Kanoi, B.N., Nagaoka, H., Miura, T., Ito, D., Takeda, H., Tsuboi, T., Takashima, E., and Otsuki, H. (2021). *Plasmodium yoelii* Erythrocyte Binding Like Protein Interacts With Basigin, an Erythrocyte Surface Protein. Front. Cell. Infect. Microbiol. *11*, 656620.
11. Aniweh, Y., Gao, X., Hao, P., Meng, W., Lai, S.K., Gunalan, K., Chu, T.T., Sinha, A., Lescar, J., Chandramohanadas, R., et al. (2017). P. falciparum RH5-Basigin interaction induces changes in the cytoskeleton of the host RBC. Cell Microbiol. *19*, e12747.
12. Yahata, K., Hart, M.N., Davies, H., Asada, M., Wassmer, S.C., Templeton, T.J., Treeck, M., Moon, R.W., and Kaneko, O. (2021). Gliding motility of *Plasmodium* merozoites. Proc. Natl. Acad. Sci. USA *118*, e2114442118.
13. Bogdanova, A., Makhro, A., Wang, J., Lipp, P., and Kaestner, L. (2013). Calcium in red blood cells-a perilous balance. Int. J. Mol. Sci. *14*, 9848–9872.
14. Kostova, E.B., Beuger, B.M., Klei, T.R.L., Halonen, P., Lieftink, C., Beijersbergen, R., van den Berg, T.K., and van Bruggen, R. (2015). Identification of signalling cascades involved in red blood cell shrinkage and vesiculation. Biosci. Rep. *35*, e00187.
15. Semenov, A.N., Shirshin, E.A., Muravyov, A.V., and Priezzhev, A.V. (2019). The Effects of Different Signaling Pathways in Adenylyl Cyclase Stimulation on Red Blood Cells Deformability. Front. Physiol. *10*, 923.
16. Eaton, J.W., Skelton, T.D., Swofford, H.S., Kolpin, C.E., and Jacob, H.S. (1973). Elevated erythrocyte calcium in sickle cell disease. Nature *246*, 105–106.

17. Ahuja, M., Jha, A., Maléth, J., Park, S., and Muallem, S. (2014). cAMP and Ca^{2+} signaling in secretory epithelia: crosstalk and synergism. Cell Calcium *55*, 385–393.
18. Kamp, T.J., and Hell, J.W. (2000). Regulation of cardiac L-type calcium channels by protein kinase A and protein kinase C. Circ. Res. *87*, 1095–1102.
19. Nystoriak, M.A., Nieves-Cintrón, M., Patriarchi, T., Buonarati, O.R., Prada, M.P., Morotti, S., Grandi, E., Fernandes, J.D.S., Forbush, K., Hofmann, F., et al. (2017). Ser1928 phosphorylation by PKA stimulates the L-type Ca2+ channel CaV1.2 and vasoconstriction during acute hyperglycemia and diabetes. Sci. Signal. *10*, eaaf9647.
20. Horga, J.F., Gisbert, J., De Agustín, J.C., Hernández, M., and Zapater, P. (2000). A beta-2-adrenergic receptor activates adenylate cyclase in human erythrocyte membranes at physiological calcium plasma concentrations. Blood Cells Mol. Dis. *26*, 223–228.
21. Neves, S.R., Ram, P.T., and Iyengar, R. (2002). G protein pathways. Science *296*, 1636–1639.
22. Seifert, R., Lushington, G.H., Mou, T.-C., Gille, A., and Sprang, S.R. (2012). Inhibitors of membranous adenylyl cyclases. Trends Pharmacol. Sci. *33*, 64–78.
23. Taylor, S.S., Kim, C., Cheng, C.Y., Brown, S.H.J., Wu, J., and Kannan, N. (2008). Signaling through cAMP and cAMP-dependent protein kinase: diverse strategies for drug design. Biochim. Biophys. Acta *1784*, 16–26.
24. Oonishi, T., Sakashita, K., and Uyesaka, N. (1997). Regulation of red blood cell filterability by Ca2+ influx and cAMP-mediated signaling pathways. Am. J. Physiol. *273*, C1828–C1834.
25. Gauthier, E., Guo, X., Mohandas, N., and An, X. (2011). Phosphorylation-dependent perturbations of the 4.1R-associated multiprotein complex of the erythrocyte membrane. Biochemistry *50*, 4561–4567.
26. George, A., Pushkaran, S., Li, L., An, X., Zheng, Y., Mohandas, N., Joiner, C.H., and Kalfa, T.A. (2010). Altered phosphorylation of cytoskeleton proteins in sickle red blood cells: the role of protein kinase C, Rac GTPases, and reactive oxygen species. Blood Cells Mol. Dis. *45*, 41–45.
27. Iyer, J., Grüner, A.C., Rénia, L., Snounou, G., and Preiser, P.R. (2007). Invasion of host cells by malaria parasites: a tale of two protein families. Mol. Microbiol. *65*, 231–249.
28. Singh, S., Alam, M.M., Pal-Bhowmick, I., Brzostowski, J.A., and Chitnis, C.E. (2010). Distinct external signals trigger sequential release of apical organelles during erythrocyte invasion by malaria parasites. PLoS Pathog. *6*, e1000746.
29. Weiss, G.E., Gilson, P.R., Taechalertpaisarn, T., Tham, W.H., de Jong, N.W.M., Harvey, K.L., Fowkes, F.J.I., Barlow, P.N., Rayner, J.C., Wright, G.J., et al. (2015). Revealing the sequence and resulting cellular morphology of receptor-ligand interactions during Plasmodium falciparum invasion of erythrocytes. PLoS Pathog. *11*, e1004670.
30. Johnson, J.G., Epstein, N., Shiroishi, T., and Miller, L.H. (1980). Factors affecting the ability of isolated Plasmodium knowlesi merozoites to attach to and invade erythrocytes. Parasitology *80*, 539–550.
31. Iancu, R.V., Ramamurthy, G., Warrier, S., Nikolaev, V.O., Lohse, M.J., Jones, S.W., and Harvey, R.D. (2008). Cytoplasmic cAMP concentrations in intact cardiac myocytes. Am. J. Physiol. Cell Physiol. *295*, C414–C422.
32. Sudlow, L.C., and Gillette, R. (1997). Cyclic AMP levels, adenylyl cyclase activity, and their stimulation by serotonin quantified in intact neurons. J. Gen. Physiol. *110*, 243–255.
33. Mironov, S.L., Skorova, E., Taschenberger, G., Hartelt, N., Nikolaev, V.O., Lohse, M.J., and Kügler, S. (2009). Imaging cytoplasmic cAMP in mouse brainstem neurons. BMC Neurosci. *10*, 29.
34. Bernhardt, I., Nguyen, D.B., Wesseling, M.C., and Kaestner, L. (2019). Intracellular Ca2+ Concentration and Phosphatidylserine Exposure in Healthy Human Erythrocytes in Dependence on in vivo Cell Age. Front. Physiol. *10*, 1629.
35. Bratosin, D., Estaquier, J., Petit, F., Arnoult, D., Quatannens, B., Tissier, J.P., Slomianny, C., Sartiaux, C., Alonso, C., Huart, J.J., et al. (2001). Programmed cell death in mature erythrocytes: a model for investigating death effector pathways operating in the absence of mitochondria. Cell Death Differ. *8*, 1143–1156.
36. Ugurel, E., Goksel, E., Cilek, N., Kaga, E., and Yalcin, O. (2022). Proteomic Analysis of the Role of the Adenylyl Cyclase-cAMP Pathway in Red Blood Cell Mechanical Responses. Cells *11*, 1250.
37. Ayoub, M.A., Damian, M., Gespach, C., Ferrandis, E., Lavergne, O., De Wever, O., Banères, J.L., Pin, J.P., and Prévost, G.P. (2009). Inhibition of heterotrimeric G protein signaling by a small molecule acting on Galpha subunit. J. Biol. Chem. *284*, 29136–29145.
38. Bitterman, J.L., Ramos-Espiritu, L., Diaz, A., Levin, L.R., and Buck, J. (2013). Pharmacological distinction between soluble and transmembrane adenylyl cyclases. J. Pharmacol. Exp. Therapeut. *347*, 589–598.
39. Swierczewski, B.E., and Davies, S.J. (2009). A schistosome cAMP-dependent protein kinase catalytic subunit is essential for parasite viability. PLoS Neglected Trop. Dis. *3*, e505.
40. Catterall, W.A., and Swanson, T.M. (2015). Structural Basis for Pharmacology of Voltage-Gated Sodium and Calcium Channels. Mol. Pharmacol. *88*, 141–150.
41. Mukai, H., Munekata, E., and Higashijima, T. (1992). protein antagonists. A novel hydrophobic peptide competes with receptor for G protein binding. J. Biol. Chem. *267*, 16237–16243.
42. Somvanshi, R.K., Chaudhari, N., Qiu, X., and Kumar, U. (2011). Heterodimerization of β2 adrenergic receptor and somatostatin receptor 5: Implications in modulation of signaling pathway. J. Mol. Signal. *6*, 9.
43. Guo, C., Li, J., Myatt, L., Zhu, X., and Sun, K. (2010). Induction of Galphas contributes to the paradoxical stimulation of cytosolic phospholipase A2alpha expression by cortisol in human amnion fibroblasts. Mol. Endocrinol. *24*, 1052–1061.
44. Tesmer, J.J., Dessauer, C.W., Sunahara, R.K., Murray, L.D., Johnson, R.A., Gilman, A.G., and Sprang, S.R. (2000). Molecular basis for P-site inhibition of adenylyl cyclase. Biochemistry *39*, 14464–14471.
45. Chu, H.-Y., Ito, W., Li, J., and Morozov, A. (2012). Target-specific suppression of GABA release from parvalbumin interneurons in the basolateral amygdala by dopamine. J. Neurosci. *32*, 14815–14820.
46. Dalton, G.D., and Dewey, W.L. (2006). Protein kinase inhibitor peptide (PKI): a family of endogenous neuropeptides that modulate neuronal cAMP-dependent protein kinase function. Neuropeptides *40*, 23–34.
47. Glass, D.B., Cheng, H.C., Mende-Mueller, L., Reed, J., and Walsh, D.A. (1989). Primary structural determinants essential for potent inhibition of cAMP-dependent protein kinase by inhibitory peptides corresponding to the active portion of the heat-stable inhibitor protein. J. Biol. Chem. *264*, 8802–8810.
48. Zhang, S., Zhou, Z., Gong, Q., Makielski, J.C., and January, C.T. (1999). Mechanism of block and identification of the verapamil binding domain to HERG potassium channels. Circ. Res. *84*, 989–998.
49. Harada, K., Ito, M., Wang, X., Tanaka, M., Wongso, D., Konno, A., Hirai, H., Hirase, H., Tsuboi, T., and Kitaguchi, T. (2017). Red fluorescent protein-based cAMP indicator applicable to optogenetics and in vivo imaging. Sci. Rep. *7*, 7351.
50. Yang, N.J., and Hinner, M.J. (2015). Getting across the cell membrane: an overview for small molecules, peptides, and proteins. Methods Mol. Biol. *1266*, 29–53.
51. Kitaguchi, T., Oya, M., Wada, Y., Tsuboi, T., and Miyawaki, A. (2013). Extracellular calcium influx activates adenylate cyclase 1 and potentiates insulin secretion in MIN6 cells. Biochem. J. *450*, 365–373.
52. Cura, V., Gangloff, M., Eiler, S., Moras, D., and Ruff, M. (2008). Cleaved thioredoxin fusion protein enables the crystallization of poorly soluble ERalpha in complex with synthetic ligands. Acta Crystallogr., Sect. F: Struct. Biol. Cryst. Commun. *64*, 54–57.
53. Murphy, S.C., Hiller, N.L., Harrison, T., Lomasney, J.W., Mohandas, N., and Haldar, K. (2006). Lipid rafts and malaria parasite infection of erythrocytes. Mol. Membr. Biol. *23*, 81–88.
54. Perrin, A.J., Patel, A., Flueck, C., Blackman, M.J., and Baker, D.A. (2020). cAMP signalling and its role in host cell invasion by malaria parasites. Curr. Opin. Microbiol. *58*, 69–74.
55. Gao, X., Gunalan, K., Yap, S.S.L., and Preiser, P.R. (2013). Triggers of key calcium signals during erythrocyte invasion by Plasmodium falciparum. Nat. Commun. *4*, 2862.
56. Jaeger, S., Igea, A., Arroyo, R., Alcalde, V., Canovas, B., Orozco, M., Nebreda, A.R., and Aloy, P. (2017). Quantification of Pathway Cross-talk Reveals Novel Synergistic Drug Combinations for Breast Cancer. Cancer Res. *77*, 459–469.
57. Willoughby, D., and Cooper, D.M.F. (2007). Organization and Ca2+ regulation of adenylyl cyclases in cAMP microdomains. Physiol. Rev. *87*, 965–1010.
58. Musumeci, G., Bon, I., Lembo, D., Cagno, V., Re, M.C., Signoretto, C., Diani, E., Lopalco, L., Pastori, C., Martin, L., et al. (2017). M48U1 and Tenofovir combination synergistically inhibits HIV infection in activated PBMCs and human cervicovaginal histocultures. Sci. Rep. *7*, 41018.
59. Wang, R., Lai, T.P., Gao, P., Zhang, H., Ho, P.L., Woo, P.C.Y., Ma, G., Kao, R.Y.T., Li, H., and Sun, H. (2018). Bismuth antimicrobial drugs serve as broad-spectrum metallo-β-lactamase inhibitors. Nat. Commun. *9*, 439.
60. Gaur, D., and Chitnis, C.E. (2011). Molecular interactions and signaling mechanisms

during erythrocyte invasion by malaria parasites. Curr. Opin. Microbiol. *14*, 422–428.
61. Cowman, A.F., Tonkin, C.J., Tham, W.-H., and Duraisingh, M.T. (2017). The Molecular Basis of Erythrocyte Invasion by Malaria Parasites. Cell Host Microbe *22*, 232–245.
62. Crosnier, C., Bustamante, L.Y., Bartholdson, S.J., Bei, A.K., Theron, M., Uchikawa, M., Mboup, S., Ndir, O., Kwiatkowski, D.P., Duraisingh, M.T., et al. (2011). Basigin is a receptor essential for erythrocyte invasion by Plasmodium falciparum. Nature *480*, 534–537.
63. Mohring, F., Hart, M.N., Rawlinson, T.A., Henrici, R., Charleston, J.A., Diez Benavente, E., Patel, A., Hall, J., Almond, N., Campino, S., et al. (2019). Rapid and iterative genome editing in the malaria parasite Plasmodium knowlesi provides new tools for *P. vivax* research. Elife *8*, e45829.
64. Satchwell, T.J., Wright, K.E., Haydn-Smith, K.L., Sánchez-Román Terán, F., Moura, P.L., Hawksworth, J., Frayne, J., Toye, A.M., and Baum, J. (2019). Genetic manipulation of cell line derived reticulocytes enables dissection of host malaria invasion requirements. Nat. Commun. *10*, 3806.
65. Maïssa, N., Covarelli, V., Janel, S., Durel, B., Simpson, N., Bernard, S.C., Pardo-Lopez, L., Bouzinba-Ségard, H., Faure, C., Scott, M.G.H., et al. (2017). Strength of Neisseria meningitidis binding to endothelial cells requires highly-ordered CD147/β2-adrenoceptor clusters assembled by alpha-actinin-4. Nat. Commun. *8*, 15764.
66. Kanjee, U., Grüring, C., Chaand, M., Lin, K.M., Egan, E., Manzo, J., Jones, P.L., Yu, T., Barker, R., Jr., Weekes, M.P., and Duraisingh, M.T. (2017). CRISPR/Cas9 knockouts reveal genetic interaction between strain-transcendent erythrocyte determinants of Plasmodium falciparum invasion. Proc. Natl. Acad. Sci. USA *114*, E9356–E9365.
67. Zenonos, Z.A., Dummler, S.K., Müller-Sienerth, N., Chen, J., Preiser, P.R., Rayner, J.C., and Wright, G.J. (2015). Basigin is a druggable target for host-oriented antimalarial interventions. J. Exp. Med. *212*, 1145–1151.
68. Sassone-Corsi, P. (2012). The cyclic AMP pathway. Cold Spring Harbor Perspect. Biol. *4*, a011148.
69. Patel, A., Perrin, A.J., Flynn, H.R., Bisson, C., Withers-Martinez, C., Treeck, M., Flueck, C., Nicastro, G., Martin, S.R., Ramos, A., et al. (2019). Cyclic AMP signalling controls key components of malaria parasite host cell invasion machinery. PLoS Biol. *17*, e3000264.
70. Dawn, A., Singh, S., More, K.R., Siddiqui, F.A., Pachikara, N., Ramdani, G., Langsley, G., and Chitnis, C.E. (2014). The central role of cAMP in regulating Plasmodium falciparum merozoite invasion of human erythrocytes. PLoS Pathog. *10*, e1004520.
71. Flueck, C., Drought, L.G., Jones, A., Patel, A., Perrin, A.J., Walker, E.M., Nofal, S.D., Snijders, A.P., Blackman, M.J., and Baker, D.A. (2019). Phosphodiesterase beta is the master regulator of cAMP signalling during malaria parasite invasion. PLoS Biol. *17*, e3000154.
72. Zaccolo, M., Zerio, A., and Lobo, M.J. (2021). Subcellular Organization of the cAMP Signaling Pathway. Pharmacol. Rev. *73*, 278–309.
73. Adderley, S.P., Sprague, R.S., Stephenson, A.H., and Hanson, M.S. (2010). Regulation of cAMP by phosphodiesterases in erythrocytes. Pharmacol. Rep. *62*, 475–482.
74. Ramasamy, R. (2014). Zoonotic malaria - global overview and research and policy needs. Front. Public Health *2*, 123.
75. Antinori, S., Galimberti, L., Milazzo, L., and Corbellino, M. (2013). Plasmodium knowlesi: the emerging zoonotic malaria parasite. Acta Trop. *125*, 191–201.
76. Davidson, G., Chua, T.H., Cook, A., Speldewinde, P., and Weinstein, P. (2019). Defining the ecological and evolutionary drivers of Plasmodium knowlesi transmission within a multi-scale framework. Malar. J. *18*, 66.
77. Hang, J.-W., Tukijan, F., Lee, E.Q.H., Abdeen, S.R., Aniweh, Y., and Malleret, B. (2021). Zoonotic Malaria: Non-Laverania Plasmodium Biology and Invasion Mechanisms. Pathogens *10*, 889.
78. Carlton, J.M., and Sullivan, S.A. (2017). A Feast of Malaria Parasite Genomes. Cell Host Microbe *21*, 310–312.
79. Chitnis, C.E., Chaudhuri, A., Horuk, R., Pogo, A.O., and Miller, L.H. (1996). The domain on the Duffy blood group antigen for binding Plasmodium vivax and P. knowlesi malarial parasites to erythrocytes. J. Exp. Med. *184*, 1531–1536.
80. Duraisingh, M.T., Maier, A.G., Triglia, T., and Cowman, A.F. (2003). Erythrocyte-binding antigen 175 mediates invasion in Plasmodium falciparum utilizing sialic acid-dependent and -independent pathways. Proc. Natl. Acad. Sci. USA *100*, 4796–4801.
81. Gao, X., Yeo, K.P., Aw, S.S., Kuss, C., Iyer, J.K., Genesan, S., Rajamanonmani, R., Lescar, J., Bozdech, Z., and Preiser, P.R. (2008). Antibodies targeting the PfRH1 binding domain inhibit invasion of Plasmodium falciparum merozoites. PLoS Pathog. *4*, e1000104.
82. Lobo, C.-A., Rodriguez, M., Reid, M., and Lustigman, S. (2003). Glycophorin C is the receptor for the Plasmodium falciparum erythrocyte binding ligand PfEBP-2 (baebl). Blood *101*, 4628–4631.
83. Aniweh, Y., Gao, X., Gunalan, K., and Preiser, P.R. (2016). PfRH2b specific monoclonal antibodies inhibit merozoite invasion. Mol. Microbiol. *102*, 386–404.
84. Pasini, E.M., Kirkegaard, M., Mortensen, P., Mann, M., and Thomas, A.W. (2010). Deep-coverage rhesus red blood cell proteome: a first comparison with the human and mouse red blood cell. Blood Transfus *8*, s126–s139.
85. Cserne Szappanos, H., Muralidharan, P., Ingley, E., Petereit, J., Millar, A.H., and Hool, L.C. (2017). Identification of a novel cAMP dependent protein kinase A phosphorylation site on the human cardiac calcium channel. Sci. Rep. *7*, 15118.
86. Mitterdorfer, J., Froschmayr, M., Grabner, M., Moebius, F.F., Glossmann, H., and Striessnig, J. (1996). Identification of PK-A phosphorylation sites in the carboxyl terminus of L-type calcium channel alpha 1 subunits. Biochemistry *35*, 9400–9406.
87. Sang, L., Dick, I.E., and Yue, D.T. (2016). Protein kinase A modulation of CaV1.4 calcium channels. Nat. Commun. *7*, 12239.
88. Kanekura, T., Miyauchi, T., Tashiro, M., and Muramatsu, T. (1991). Basigin, a new member of the immunoglobulin superfamily: genes in different mammalian species, glycosylation changes in the molecule from adult organs and possible variation in the N-terminal sequences. Cell Struct. Funct. *16*, 23–30.
89. Köpnick, A.-L., Jansen, A., Geistlinger, K., Epalle, N.H., and Beitz, E. (2021). Basigin drives intracellular accumulation of l-lactate by harvesting protons and substrate anions. PLoS One *16*, e0249110.
90. Muramatsu, T. (2016). Basigin (CD147), a multifunctional transmembrane glycoprotein with various binding partners. J. Biochem. *159*, 481–490.
91. Muramatsu, T., and Miyauchi, T. (2003). Basigin (CD147): a multifunctional transmembrane protein involved in reproduction, neural function, inflammation and tumor invasion. Histol. Histopathol. *18*, 981–987.
92. Wang, K., Chen, W., Zhang, Z., Deng, Y., Lian, J.Q., Du, P., Wei, D., Zhang, Y., Sun, X.X., Gong, L., et al. (2020). CD147-spike protein is a novel route for SARS-CoV-2 infection to host cells. Signal Transduct. Targeted Ther. *5*, 283.
93. Harrison, T., Samuel, B.U., Akompong, T., Hamm, H., Mohandas, N., Lomasney, J.W., and Haldar, K. (2003). Erythrocyte G protein-coupled receptor signaling in malarial infection. Science *301*, 1734–1736.
94. Moon, R.W., Hall, J., Rangkuti, F., Ho, Y.S., Almond, N., Mitchell, G.H., Pain, A., Holder, A.A., and Blackman, M.J. (2013). Adaptation of the genetically tractable malaria pathogen Plasmodium knowlesi to continuous culture in human erythrocytes. Proc. Natl. Acad. Sci. USA *110*, 531–536.
95. Trager, W., and Jensen, J.B. (1976). Human malaria parasites in continuous culture. Science *193*, 673–675.
96. Ngernna, S., Chim-Ong, A., Roobsoong, W., Sattabongkot, J., Cui, L., and Nguitragool, W. (2019). Efficient synchronization of Plasmodium knowlesi in vitro cultures using guanidine hydrochloride. Malar. J. *18*, 148.
97. Huang, X., Huang, S., Ong, L.C., Lim, J.C.S., Hurst, R.J.M., Mushunje, A.T., Matsudaira, P.T., Han, J., and Preiser, P.R. (2016). Differential Spleen Remodeling Associated with Different Levels of Parasite Virulence Controls Disease Outcome in Malaria Parasite Infections. mSphere *1*, e00018-15.
98. Huang, X., Liew, K., Natalang, O., Siau, A., Zhang, N., and Preiser, P.R. (2013). The role of serine-type serine repeat antigen in Plasmodium yoelii blood stage development. PLoS One *8*, e60723.
99. Paone, S., D'Alessandro, S., Parapini, S., Celani, F., Tirelli, V., Pourshaban, M., and Olivieri, A. (2020). Characterization of the erythrocyte GTPase Rac1 in relation to Plasmodium falciparum invasion. Sci. Rep. *10*, 22054.
100. Söderberg, O., Gullberg, M., Jarvius, M., Ridderstråle, K., Leuchowius, K.J., Jarvius, J., Wester, K., Hydbring, P., Bahram, F., Larsson, L.G., and Landegren, U. (2006). Direct observation of individual endogenous protein complexes in situ by proximity ligation. Nat. Methods *3*, 995–1000.

STAR★METHODS

KEY RESOURCES TABLE

REAGENT or RESOURCE	SOURCE	IDENTIFIER
Antibodies		
Mouse anti-His antibody	Qiagen	34660; RRID: AB_2313733
mAb Ab-1 Fab fragment	Absolute Antibody	Ab00524-10.6; RRID: AB_2313733
mAb C41	Gao et al.[55]	N/A
mAb RH5(7)	Aniweh et al.[11]	N/A
Rabbit anti-CD147 antibody	Axil Scientific	A304-489A; RRID: AB_2313733
Rabbit anti-CD44 antibody	Abcam	ab157107; RRID: AB_2313733
β2-Adrenergic Receptor (D6H2) Rabbit mAb	Cell Signaling Technology	8513s; RRID: AB_2313733
Rabbit anti-DARC antibody	Abcam	ab137044; RRID: AB_2313733
Mouse IgG HRP Linked Whole Ab	Cytiva	GENA931-1ML; RRID: AB_2313733
Rabbit IgG HRP Linked Whole Ab	Cytiva	GENA934-1ML; RRID: AB_2313733
Mouse anti-HA	Invitrogen	26183; RRID: AB_2313733
Goat anti-Rabbit IgG (H + L) Cross-Adsorbed Secondary Antibody, Alexa Fluor™ 488	Invitrogen	A-11008; RRID: AB_2313733
IRDye 800CW Goat anti-Mouse IgG Secondary Antibody	LI-COR Biosciences	LIR.926-32210; RRID: AB_2313733
Chemicals, peptides, and recombinant proteins		
RPMI1640	Gibco	23400062
Giemsa stain	Sigma	GS1L
Percoll	MP biochemicals	0219536990
Histodenz™	Sigma	D2158
Guanidine hydrochloride	Sigma	50950
E64	Sigma	E3132
EGTA	1st Base	CUS-1070
Na2HPO4	Merck	567547-1KG
NaH2PO4	Merck	04269-1KG
K2HPO4	Merck	P3786
ATP	Merck	A1852
KOAc	Merck	W292001
MgCl2	Merck	M8266
KCl	Merck	P4504
NaCl	Sigma	106404
Phosphate buffered saline (PBS)	Axil Scientific	BUF-204010X1L
Isopropyl-β-d-thiogalactopyranoside (IPTG)	Sigma	16758
HEPES	Sigma	H4034
Forskolin	Abcam	ab120058
PierceTM IP lysis buffer	Thermo Scientific	87788
Isopore polycarbonate membrane	Merck	GTTP04700
Nitrocellulose membranes (0.2 μm)	Bio-Rad	1620112
Immno-Blot Low Fluorescence PVDF membrane (0.45 μM)	Bio-Rad	1620264
PBS blocking buffer	LI-COR Biosciences	LIR.927-70003

(*Continued on next page*)

Continued

REAGENT or RESOURCE	SOURCE	IDENTIFIER
Fluo-4 AM	Invitrogen	F14201
Cytochalasin D	Sigma	C8273-1MG
cOmplete His-Tag purification Resin	Merck	5893682001
Imidazole	Merck	I2399-500G
Bovine serum albumin	Sigma	A3608
Sodium Dodecyl Sulfate (SDS)	Sigma	436143
Coomassie Brilliant blue G 250	Sigma	1.15444
Influenza Hemagglutinin (HA) peptide	Sigma	I2149-1MG
BIM46187	MedChem Express	HY-10499
2′,5′-Dideoxy-adenosine	Sigma	D7408
PKA (14-22)	Sigma	P9115-1MG
Verapamil	Sigma	V4629
G Protein antagonist peptide	Sigma	G9541
NF449	Santa Cruz Biotechnology	sc-478179
2′-Deoxy-adenosine 3′-monophosphate	Santa Cruz Biotechnology	sc-216288
Rp-8-OH-cAMPS	Santa Cruz Biotechnology	sc-391035
PKA (6-22)	Sigma	P6062-1MG
N-methyl verapamil	Abcam	ab147459
Recombinant RH5	Aniweh et al., 2017	N/A
Recombinant Pink Flamindo	NTU Protein Purification platform	N/A
Critical commercial assays		
cAMP Assay Kit (Competitive ELISA)	Abcam	ab65355
SuperSignalTM West Pico PLUS Chemiluminescence Substrate	Thermo Scientific	34578
NaveniFlex Cell MR RED	Research Instruments	NC.MR.100.RED
Experimental models: Organisms/strains		
P. falciparum 3D7	MR4	N/A
P. knowlesi A1-H.1	Moon et al.[94]	N/A
P. yoelii yoelii YM	MR4	N/A
BALB/cAnNTac, Male, 5–6 weeks	Invivos	N/A
Recombinant DNA		
Pink Flamindo Plasmid	Addgene	102356
Software and algorithms		
Prism	GraphPad	N/A
TECAN-i-control 1.8.20.0	TECAN	N/A
Zen black	Carl Zeiss	N/A
DP Controller 2.2.1.227 imaging software	Olympus	N/A
One-way ANOVA	Excel	N/A
Adobe Photoshop CS6	Adobe	N/A

EXPERIMENTAL MODEL AND STUDY PARTICIPANT DETAILS

Human subjects

The human whole blood was donated by healthy non-malarial immune male adult volunteers at either the National University Hospital, Singapore or Fullerton Healthcare at Nanyang Technological University. Donors were required to be between the ages of 21–65 years old. Informed consent given was written. Informed consents were obtained from all donors in accordance with protocols approved by

Institutional Review Board of Nanyang Technological University, Singapore (IRB-2018-02-031, IRB-2019–09-047, IRB-2019–09-042 and IRB-2020-11-047). Ancestry, race, ethnicity, and socioeconomic status were not taken into consideration for this study.

Animal subjects

The peripheral blood was collected from a healthy male macaque (born in 2012) in Singapore Experimental Medical Center, Singapore with an Institutional Animal Care and Use Committees prior (IACUC) approved by the SingHealth Institutional Animal Care and Use Committee. All animals were housed in accordance with the Guide for the Care and Use of Laboratory Animals and the Association for the Assessment and Accreditation of Laboratory Animal Care (AAALAC) Standards. All efforts were made to minimise the suffering.

BALB/cN male mice of 5–6 weeks old (Invivos) were used in this study. All animal work was carried out in strict accordance with the recommendations of the NACLAR (National Advisory Committee for Laboratory Animal Research) guidelines under the Animal & Birds (Care and Use of Animals for Scientific Purposes) Rules of Singapore. The protocol was approved by the Institutional Animal Care and Use Committee of Nanyang Technological University, Singapore (Approval number: A21065). All efforts were made to minimise the suffering.

Parasite culture and isolation of schizonts and/or merozoites

P. falciparum parasite strains 3D7 (MR4) were cultured in fresh RBCs in a cRPMI with 5%CO2/3%O2/N2.[95] Mature schizonts were purified via 68% percoll (MP biochemical)[81] and treated with 10 μM E64 (Sigma). Pellet containing E64-treated schizonts were resuspended in cRPMI medium and filtered through a 2 μm Isopore polycarbonate membrane (Sigma) to purify free merozoites.

P. knowlesi parasite strain A1-H.1 were cultured in fresh RBCs from healthy human donors or macaques with 5%CO2/3%O2/N2.[94] Parasite culture was synchronised at the early ring stage with guanidine hydrochloride (GuHCl) (Sigma).[96] Schizonts were harvested by Nycodenz (Sigma) density gradient centrifugation.[94] Merozoites were isolated as mentioned above. BALB/cN mice (InVivos) were infected with *P. yoelii* YM parasites by intraperitoneal injections as previously described.[97] Schizont stage parasites were separated and harvested using a 50–60% Histodenz (Sigma) density gradient centrifugation.[98]

METHOD DETAILS

Generation and purification of recombinant RH5 protein

Recombinant RH5 protein was generated as a His-tag fusion protein and purified via size-exclusion chromatography (SEC) according to manufacturer's protocol.[11] The purity of rRH5 was confirmed by 10% SDS-PAGE followed by Coomassie blue staining (Sigma) and western blot.

Erythrocyte binding assay

The binding assay of recombinant RH5 protein to 100 μL packed normal RBC was carried out at 37°C for 1 h. Proteins bound to the RBCs were eluted by incubation with 20 μL of 1.5 M NaCl (Sigma).[11,55]

Generation of RBC ghosts

Fresh RBC pellets were split into two sets: One set of pellets is kept on ice. The other set is incubated with 0.2 mg/mL rRH5 in RPMI medium in the absence and presence of 0.5 μg/mL anti-basigin mAb Ab-1 Fab fragment (Absolute Antibody) or 0.2 mg/mL RH1 inhibitory mAb C41,[11,55] respectively. Subsequently, the two sets of pellets were lysed in 1x hypotonic lysis buffer comprising of 1.43 mM Na_2PO4 and 5.7 mM Na_2HPO_4 to form RBC ghost. The RBC ghost pellets in both sets were washed multiple times with 1x hypotonic lysis buffer to remove the hemoglobin as much as possible followed by solubilised in IP lysis buffer containing 25 mM Tris-HCl pH 7.4, 150 mM NaCl, 1 mM EDTA, 1% NP-40 and 5% glycerol (Thermo Scientific). This buffer has been successfully applied for RBC membrane extraction.[99] Solubilised rRH5-bound RBC ghosts were subsequently incubated with Ni-NTA beads for the affinity purification of His-tagged rRH5-bound RBC ghost proteins. Ni-NTA beads were resuspended in 500 mM imidazole to elute the rRH5-bound RBC ghost proteins. All samples were stored at −80°C for further studies.

Western blot analysis of RBC ghosts

Unbound RBC ghosts were separated on 10% SDS-PAGE. RH5-bound and unbound RBC ghosts were separated on 5% Native-PAGE. The gels were transferred onto nitrocellulose membranes (0.2 μm) (Bio-Rad) and probed with basigin, CD44 and β2AR antibodies (Abcam) at 1:2,000 dilution, respectively, followed by HRP-linked secondary antibodies (1:5,000) and enhanced chemiluminescence (GE healthcare). α-His antibody (Qiagen) was used at 1:5,000 dilution to detect the presence of rRH5 in Native-PAGE.

Proximity ligation assay (PLA)

PLA enables *in situ* detection of protein-protein interactions at endogenous protein levels.[100] The assay was performed according to manufacturer's protocol (Navinci). The glass slides with the blood smears of RBC only and RH5-bound RBC in the absence and presence of mAb RH5(7) were dually probed with α-His and α-basigin, α-His and α-CD44, α-His and α-β2AR, or α-His and α-DARC (negative control) (Abcam). The slides were then probed with corresponding secondary antibodies conjugated with either plus or minus PLA probes. The staining was performed following manufacturer's protocol. Fluorescence images were captured with excitation at 561 nm and emission at 590 nm

using Zeiss Live Cell Observer II Microscope (Carl Zeiss) under 100× objective lens. The PLA signal was visualised as red fluorescent dots. The fluorescence images were processed using Zen black software (Carl Zeiss).

Immunofluorescence assay and microscopy

RBCs were fixed with 4% PFA (Thermo Scientific) and incubated with α-DARC (1:100) for 1 h in 3% BSA/PBS buffer and washed in RPMI three times. The cells were then incubated with Alexa Flour 488 anti-rabbit secondary antibody (1:1,000) (Invitrogen) for 1 h. RBCs were washed in RPMI three times and resuspended with RPMI in an 8-well chamber slide (ibidi). The fluorescence images were captured using a Zeiss Live Cell Observer II Microscope (Carl Zeiss) under 100× objective lens. The fluorescence images were processed using Zen black software (Carl Zeiss).

Generation of resealed RBC with membrane-impermeable signaling inhibitors

Fresh RBCs were lysed in lysis buffer containing 5 mM K_2HPO_4 and 1mM ATP and resealed in 475 mM KOAC, 25 mM Na_2HPO_4, 25 mM $MgCl_2$ and 237.5 mM KCl.[53] Membrane-impermeable inhibitors (Table 1) including Influenza Hemagglutinin (HA) peptide (Sigma) used in this study were dissolved in water. During lysis, membrane-impermeable inhibitors were added, respectively. HA peptide was added into a separate set as an internal control.

cAMP immunoassay

The dynamic changes of cAMP levels in RBCs were performed by using the cAMP Direct Immunoassay Kit (Abcam) following Abcam's protocol. The optical density at 450 nm were measured with BioTek Cytation 5 Cell Imaging Multi-Mode Reader (Agilent). 10 μL RBCs were incubated in the absence and presence of recombinant RH5 protein (0.2 mg/mL) in a total volume of 100 μL in 1x phosphate buffered saline (PBS) and measured at different duration of 0, 2, 4, 6, 8, and 10 min 50 μM Forskolin (Abcam) was used as a positive control. Anti-basigin Fab fragment (Absolute Antibody) at 5 μg/mL, membrane-permeable inhibitor BIM46187 and 2′,5′-ddA (Table 1) at 80 μM were applied to RBCs in the presence of rRH5, respectively, and measured after 2-min incubation. rRBCs were prepared in the absence and presence of membrane-impermeable inhibitors (Table 1), respectively. rRBCs loaded with HA peptide were prepared as an internal control. cAMP level was measured mentioned above in rRBCs in the presence of rRH5 after 2-min incubation. The fold change in cAMP level in the RBC or rRBC was compared to that in RBC only or rRBC loaded with HA peptide.

Dot blot analysis of resealed RBCs

Empty rRBCs and rRBCs preloaded with HA peptide were lysed with equal volume of hypotonic lysis buffer at 4°C and centrifuged at 20,000 g for 5 min 10 μL of each lysate was properly spotted on the Immno-Blot Low Fluorescence PVDF membrane (0.45 μM) (Bio-Rad). 2 μL of 0.2 mg/mL HA peptide was directly loaded on the membrane as a positive control. The membrane was dried for 10 min at 37°C and incubated in the PBS blocking buffer (Licor) for 1 h. Specific HA signal was detected by mouse anti-HA antibody at 1:3,000 dilution, followed by anti-mouse secondary antibody Alexa Fluor 488 (Licor). Odyssey® CLx Imaging System (Licor) was used to monitor the signal of HA peptide.

Generation of Pink Flamindo protein

To prepare a soluble Pink Flamindo protein suitable for RBC loading, we have generated a recombinant N-terminal His- and thioredoxin-tagged Pink Flamindo protein. Pink Flamindo cAMP reporter sequence was amplified from pcDNA3.1-Pink Flamindo (Addgene),[49] containing a red fluorescent protein variant mApple from amino acid 1–236, in which two linker positions at amino acid 150 and 151 flanks a cAMP-binding domain derived from amino acid region 205–353 of the EPAC protein.[49] The PCR product was inserted into pNH-TrxT cloning vector and transformed into *Escherichia coli* BL21(DE3) (Stratagene) and cultured in liquid broth (MP Biomedicals) at 37°C and later induced with 0.5 mM isopropyl-β-*d*-thiogalactopyranoside (IPTG) (Sigma) at 18°C when optical density at 600 nm (OD600) reaches 2.0. Protein expression was allowed to continue overnight, and cells were harvested by centrifugation at 4,200 rpm at 15°C for 10 min. Cell pellets were lysed by sonication. The soluble fraction was purified in 20 mM HEPES and 500 mM NaCl (pH 7.5) via His-Tag purification, and further purified by Superdex 200 column (GE Healthcare). The purity of Pink Flamindo was verified by 10% SDS-PAGE followed by Coomassie blue staining (Sigma) and western blot probed with α-His antibody (1:5,000).

Viability assay of free merozoites

Merozoite viability assay was performed by adding purified merozoites as mentioned above[55] in both normal RBCs and rRBCs, respectively. Smears were prepared and stained with Giemsa (Sigma). Invasion rates were determined as (%) parasitemia. Approximately 1,000 RBCs were scored for presence of rings on Giemsa-stained smears after 24 h post-invasion. Invasion was measured as (%) parasitemia. (%) Parasitemia = (total number of ring-infected RBCs/total number of RBCs) × 100. The viability of the merozoites was confirmed by observing newly invaded rings in both set-ups.

Merozoite invasion inhibition assay with EGTA

Merozoite invasion inhibition assay was performed by adding purified late stage schizonts mentioned above into normal RBCs in the absence or presence of 2.5 mM EGTA (1st Base). Smears were prepared and stained with Giemsa (Sigma). Approximately 1,000 RBCs were scored for presence of rings on Giemsa-stained smears after 18–24 h post-invasion. Invasion was measured as (%) parasitemia. (%) Parasitemia = (total

number of ring-infected RBCs/total number of RBCs) × 100. Invasion in RBCs in the presence of EGTA was compared to that in RBCs without EGTA. Invasion inhibition efficiencies were determined as follows: (%) invasion inhibition = ((positive control-inv(EGTA)/positive control) x100).

Merozoite invasion inhibition assay with membrane-impermeable inhibitors

Membrane-impermeable inhibitors (Table 1) and was loaded in rRBCs at 2-fold increasing concentrations from 0.1953125 μM to 100 μM. Purified merozoites were added at 2% hematocrit. rRBCs pre-loaded in the absence and presence of 100 μM HA peptide were used as a positive control and an internal positive control, respectively. An invasion control experiment was performed in normal RBCs in the absence and presence of membrane-impermeable inhibitors listed in Table 1. HA peptide was added to normal RBCs as an internal control. A total of 1,000 rRBCs were scored for presence of rings on Giemsa-stained smears after 18–24 h post-invasion. Invasion was measured as (%) parasitemia. (%) Parasitemia = (total number of ring-infected rRBCs/total number of rRBCs) × 100. In the presence of inhibitor loaded into rRBCs, invasion was compared to that in rRBCs preloaded with HA peptide. Invasion inhibition efficiencies were determined as follows: (%) invasion inhibition = ((positive control-inv(inhibitor)/positive control) x100). The data was plotted by using the nonlinear curve fitting tool of GraphPad Prism.

Visualisation and measurement of RBC cAMP or Ca^{2+} by fluorescent microscopy and fluorescence plate reader

Pink Flamindo loaded rRBCs were incubated with rRH5 protein at 0.2 mg/mL in the absence and presence of anti-basigin Fab fragment (5 μg/mL) and membrane-permeable inhibitors including 80 μM BIM46187, 80 μM 2′,5′-ddA, 40 μM PKA (14–22) and 40 μM verapamil, respectively. Pink Flamindo loaded rRBCs incubated with 50 μM forskolin was used as a positive control. Fluo-4a.m. labeled (Invitrogen) normal human RBCs were incubated with rRH5 protein at 0.2 mg/mL in the absence and presence of membrane-permeable inhibitors mentioned above. The culture was applied under Nikon Eclipse Ti Inverted Microscope. 20× objective lens was used to observe and capture a wider field of RBC. The above-mentioned samples were prepared for a real-time RBC cAMP measurement or Ca^{2+} measurement using a fluorescence plate reader (Infinite M200; Tecan).[55]

Human and monkey intact RBCs labeled with 10 μM Fluo-4a.m. were incubated with either freshly purified merozoites from *P. falciparum* 3D7 or *P. knowlesi* A1-H.1. Human rRBCs labeled with 10 μM Fluo-4a.m. were incubated with either freshly purified merozoites from *P. falciparum* 3D7 or *P. knowlesi* A1-H.1 or rRH5 (0.2 mg/mL) in the absence and presence of membrane-impermeable inhibitors (Table 1) at 100 μM, respectively. rRBCs loaded with HA peptide (100 μM) was used as an internal positive control.

Time-resolved changes of cytosolic cAMP or Ca^{2+} levels inside RBCs and rRBCs were assessed using a fluorescence plate reader (Infinite M200; Tecan) and analyzed.[55] Fluorescence intensity was measured for 600 s with excitation at 565 nm and emission at 590 nm for Pink Flamindo and excitation at 488 nm and emission at 530 nm for Fluo-4a.m. by TECAN-i-control 1.8.20.0 software. The maximum increase of fluorescence (F) during a period of 600 s after the start of the stimulation was normalised to the fluorescence intensity before stimulation (F0). Changes in cytosolic cAMP or Ca^{2+} levels (ΔF(t)) were expressed as changes in fluorescence intensity as a percentage of the starting fluorescence levels: $\Delta F(t)=(F-F0)/F0$ where F = fluorescence intensity (t), F0 = starting fluorescence signal. The total changes of signals ($\sum\Delta F(t)$) in RBCs along the 600 s were summed up and plotted.

Live video microscopy

Mature schizonts of *P. falciparum* 3D7, *P. knowlesi* A1-H.1 and *P. yoelii* YM were purified and incubated with Fluo-4a.m. labeled normal human RBC, monkey RBC and mouse RBC, respectively. To analyze the effect of membrane-impermeable inhibitors (Table 1) at 100 μM on Ca^{2+} signal, mature schizonts from *P. falciparum* 3D7 and *P. knowlesi* A1-H.1 were incubated with inhibitor-loaded rRBCs that were labeled with 10 μM Fluo-4a.m. Freshly prepared rRBCs were used as a positive control. rRBCs preloaded with 100 μM HA peptide were also prepared as an internal positive control.

Samples were loaded onto a glass-bottom chamber in a cRPMI with 5%CO2/3%O2/N2 and observed under Zeiss LSM980 confocal microscope equipped with a temperature-controlled stage. Bright field and fluorescence images were captured using a 1.4NA Plan-Apo 63× oil immersion lens. Eight-bit time-lapse images of invasion events were captured, and mean fluorescence intensity within region of interest in the focal plane was determined after background subtraction using Zen black software (Carl Zeiss).

Checkerboard invasion inhibition assay

Purified *P. falciparum* 3D7 merozoites were incubated with rRBCs pre-loaded with the combinations of impermeable inhibitors (Table 1) with N-methyl Vera at 2% hematocrit. Purified merozoites incubated with rRBCs were used as positive control. Invasion inhibition was measured as mentioned in this study.[55] Invasion in the presence of inhibitors was compared with positive controls of invasion. The Minimum Inhibitory Concentration (MIC) and the Fractional Inhibitory Concentration (FIC) index were used to calculate the isobologram in Figure 6.[58,59]

Junction-arrested merozoite blocking assay

Purified *P. falciparum* 3D7 schizonts were incubated with rRBCs loaded in the absence or presence of inhibitors listed in Table 1, followed by treated with 2 μM of cytochalasin D (Cyto D). rRBCs preloaded with 100 μM HA peptide were used as a positive control. Giemsa-stained smears were prepared for counting merozoites arrested at junction formation by using light microscope. Approximately 1,000 merozoites were scored. The number of junction-arrested merozoites in the presence of impermeable inhibitors were compared that in the positive

control. Junction-arrested merozoite inhibition efficiencies were determined as follows: % junction arrested merozoite = Total number of junction arrested merozoite/Total number of RBCs × 100.

QUANTIFICATION AND STATISTICAL ANALYSIS

Samples from three independent biological replicates were used for this study. Invasion inhibition assays were performed using GraphPad Prism Version 8.0 (GraphPad Software, USA). Statistical comparison was done using one-way ANOVA as appropriate. A p value of <0.05 was considered statistically significant. The p-value is provided in individual experiment if required.